

OPTIMALLY WEIGHTED PCA FOR HIGH-DIMENSIONAL HETEROSCEDASTIC DATA

BY DAVID HONG^{*}, JEFFREY A. FESSLER[†] AND LAURA BALZANO[‡]

University of Michigan

Modern applications increasingly involve high-dimensional and heterogeneous data, e.g., datasets formed by combining numerous measurements from myriad sources. Principal Component Analysis (PCA) is a classical method for reducing dimensionality by projecting such data onto a low-dimensional subspace capturing most of their variation, but PCA does not robustly recover underlying subspaces in the presence of heteroscedastic noise. Specifically, PCA suffers from treating all data samples as if they are equally informative. This paper analyzes a weighted variant of PCA that accounts for heteroscedasticity by giving samples with larger noise variance less influence. The analysis provides expressions for the asymptotic recovery of underlying low-dimensional components from samples with heteroscedastic noise in the high-dimensional regime, i.e., for sample dimension on the order of the number of samples. Surprisingly, it turns out that whitening the noise by using inverse noise variance weights is sub-optimal. We derive optimal weights, characterize the performance of weighted PCA, and consider the problem of optimally collecting samples under budget constraints.

1. Introduction. Principal Component Analysis (PCA) is a classical method for reducing the dimensionality of data by representing them in terms of new variables, called principal components, that largely capture the meaningful variation in the data [15]. However, standard PCA is sub-optimal for data samples with varying quality since it treats all samples uniformly [11]. Weighted PCA (WPCA) addresses this shortcoming by giving less informative samples less weight. Doing so enables WPCA to better recover underlying principal components from noisy data, but choosing the best weights has been an open problem, even when data noise variances are known. This paper analyzes the performance of WPCA for heteroscedastic data, that is, for data samples with heterogeneous noise variance. We derive

^{*}Supported by NSF Graduate Research Fellowship DGE #1256260 and by NSF Grant ECCS-1508943.

[†]Supported by the UM-SJTU data science seed fund and by NIH Grant U01 EB 018753.

[‡]Supported by DARPA-16-43-D3M-FP-037 and by NSF Grant ECCS-1508943.

MSC 2010 subject classifications: Primary 62H25, 62H12; secondary 62F12

Keywords and phrases: weighted principal component analysis, high dimensional data, subspace estimation, heteroscedasticity, asymptotic random matrix theory

optimal weights for recovery of underlying components and characterize the performance of optimally weighted PCA in high-dimensional settings.

1.1. *High-dimensional and heteroscedastic data.* Modern PCA applications span numerous and diverse areas, ranging from medical imaging [2, 20] to cancer data classification [21], genetics [17], and environmental sensing [19, 26], to name just a few. Increasingly, the number of variables measured is large, i.e., comparable to or even larger than the number of samples; the data are *high-dimensional*. Traditional asymptotic results that consider performance as only the number of samples grows do not apply well to such settings. New intuitions, theory and approaches are needed for the high-dimensional regime where the number of variables grows together with the number of samples [14].

When samples are obtained under varied conditions, they will likely have varied quality. In particular, some samples will have noise of larger variance than others, i.e., the data will have *heteroscedastic noise*. For example, Cochran and Horne [6] use a type of weighted PCA because their spectrophotometric data is obtained from averages taken over increasing windows of time; samples from longer windows have lower noise variance. Similarly, astronomical measurements of stars [23] have heterogeneous amounts of noise among samples due to differing atmospheric effects from one sample to the next. Finally, modern big data inference is increasingly done using datasets built up from myriad sources, and hence one can expect heteroscedasticity will be the norm.

1.2. *Weighted Principal Component Analysis.* We consider a sample-weighted PCA [15, Section 14.2.1] to account for heteroscedastic noise in the data; giving noisier samples smaller weights reduces their influence. Sample-weighted PCA (WPCA) replaces the sample covariance matrix with a weighted sample covariance matrix $(\omega_1 y_1 y_1^H + \dots + \omega_n y_n y_n^H)/n$ where $y_1, \dots, y_n \in \mathbb{C}^d$ are zero-mean sample vectors, $\omega_1, \dots, \omega_n \geq 0$ are the weights, and the superscript H denotes Hermitian transpose. As in PCA, the principal components¹ $\hat{u}_1, \dots, \hat{u}_k \in \mathbb{C}^d$ and amplitudes $\hat{\theta}_1^2, \dots, \hat{\theta}_k^2$ are the first k eigenvectors and eigenvalues, respectively, of the weighted sample covariance matrix. The scores $\hat{z}_1, \dots, \hat{z}_k \in \mathbb{C}^n$ are given by $\hat{z}_i = (1/\hat{\theta}_i) \{\hat{u}_i^H(y_1, \dots, y_n)\}^H$ for each $i \in \{1, \dots, k\}$. Taken together, the principal components, ampli-

¹In contrast to [15], “principal components” here refers to eigenvectors of the (weighted) sample covariance matrix and “scores” refers to the derived variables, i.e., the coefficients of the samples with respect to the components.

tudes and scores solve the weighted approximation problem

$$(1) \quad \min_{\substack{\tilde{u}_1, \dots, \tilde{u}_k \in \mathbb{C}^d \\ \tilde{\theta}_1, \dots, \tilde{\theta}_k \geq 0 \\ \tilde{z}_1, \dots, \tilde{z}_k \in \mathbb{C}^n}} \sum_{j=1}^n \omega_j^2 \left\| y_j - \sum_{i=1}^k \tilde{u}_i \tilde{\theta}_i (\tilde{z}_i^{(j)})^* \right\|_2^2$$

such that $\tilde{u}_s^H \tilde{u}_t = \delta_{st}$, $\tilde{z}_s^H \mathbf{W}^2 \tilde{z}_t = n \delta_{st}$,

where $\mathbf{W} := \text{diag}(\omega_1, \dots, \omega_n)$ is a diagonal matrix of weights, and $\delta_{st} = 1$ if $s = t$ and 0 otherwise. Namely, they form a truncated generalized singular value decomposition [9, Appendix A] of the data matrix $\mathbf{Y} := (y_1, \dots, y_n) \in \mathbb{C}^{d \times n}$ formed with samples as columns. Note that the scores $\hat{z}_1, \dots, \hat{z}_k$ are orthonormal with respect to the weighted Euclidean metric \mathbf{W}^2 , and are not necessarily so with respect to the Euclidean metric. Reconstructed samples $\hat{x}_1, \dots, \hat{x}_n \in \mathbb{C}^d$ are formed for each $j \in \{1, \dots, n\}$ as

$$(2) \quad \hat{x}_j := \sum_{i=1}^k \hat{u}_i \hat{\theta}_i (\hat{z}_i^{(j)})^*,$$

and are projections of the samples y_1, \dots, y_n onto the principal component subspace, i.e., the span of $\hat{u}_1, \dots, \hat{u}_k$.

To use WPCA, one must first select weights. Some natural choices to consider for heteroscedastic data are:

- uniform weights $\omega_j^2 = 1$: standard (unweighted) PCA may be a natural choice when data are “nearly” homoscedastic, but its performance generally degrades with increasing heteroscedasticity as shown, e.g., in [11, Theorem 2].
- binary weights $\omega_j^2 = 0$ for noisier samples and $\omega_j^2 = 1$ for the rest: excluding samples that are much noisier is both practical and natural, but how much noisier they need to be is not obvious. Our analysis quantifies when doing so is nearly optimal.
- inverse noise variance weights $\omega_j^2 = 1/\eta_j^2$ where η_j^2 is the j th sample noise variance: weighting by inverse noise variance whitens the noise, making it homoscedastic, and can be interpreted as a maximum likelihood weighting [27], but given that conventional PCA is not robust to gross outliers, e.g., from very noisy samples, it is uncertain whether inverse noise variance downweights such samples aggressively enough.

It has been unclear which, if any, of these three options should be chosen, but among them inverse noise variance weights generally appear most natural, especially when all noise variances are moderate. Surprisingly, our

analysis shows that none of these options optimally recover underlying components when the data have heteroscedastic noise. In some cases, they are near optimal, and our analysis uncovers these regimes as well.

1.3. *Contributions of this paper.* This paper analyzes WPCA and characterizes, for any choice of weights, the asymptotic recovery of underlying components, amplitudes and scores from data samples with heteroscedastic noise (Theorem 1). We provide simplified expressions that allow us to obtain insights into the performance of WPCA as well as optimize the weights for various types of recovery, and we derive a surprisingly simple closed-form expression (Theorem 6) for weights that optimally recover an underlying component of amplitude θ_i : $\omega_j^2 = 1/\{\eta_j^2(\theta_i^2 + \eta_j^2)\}$. These expressions also allow us to find optimal strategies for collecting samples under budget constraints (Theorem 7). Finally, we investigate some cases where suboptimal weights may be practical and sufficient and study how weighting changes the ways that data properties, e.g., noise variances and number of samples, affect PCA performance.

1.4. *Relationship to previous works.* Jolliffe [15, Section 14.2.1] describes a more general WPCA; one may, for example, also weight the coordinates of each sample. Within-sample weighting is discussed in [7, Sections 5.4–5.5] to account for variables with differing noise variances; the weights are inverse noise variance and the authors note that it corresponds to maximum likelihood estimation for the factor analysis model [7, Equation (20)]. Weighting both across and within samples is proposed in [6, Equation (28)] for analyzing spectrophotometric data from scanning wavelength kinetics experiments. The weights in [6] are also inverse noise variance. Similar weighting is used in [23, Equation (1)] for analyzing photometric light curve data from astronomical studies, and in [13] for analyzing metabolomics data. Weighting data by their inverse noise variance has been a recurring theme, but the resulting performance has not been studied in the high-dimensional regime. This paper analyzes the high-dimensional asymptotic performance of general across-sample weighting in WPCA for noise with heteroscedasticity across samples. Generalizing the analysis of this paper to heteroscedasticity that is both across and within samples with correspondingly general weighting is an interesting area of future work.

Weighted variants of PCA have also been applied to account for other heterogeneities in the data. Jolliffe [15, Section 14.2.1] surveys and discusses several such settings, and Yue and Tomoyasu [28, Sections 3–5] use weights to account for, among other aspects, the relative importance of variables. Weighted variants of PCA are also closely tied to the problem of computing

weighted low-rank approximations of matrices; see, e.g., [22] and [25, Section 4.2], where weights are used to account for unobserved data or to denote relative importance. Understanding how to handle such heterogeneities is an exciting area for future work and will become increasingly important for big data inference from “messy” data.

Choosing uniform weights specializes WPCA to (unweighted) PCA, so the analysis here generalizes that of our previous paper [11]. There we analyzed the asymptotic recovery of PCA and characterized the impact of heteroscedastic noise, showing, in particular, that PCA performance is always best (for fixed average noise variance) when the noise is homoscedastic. See [11, Section 1.3] for a discussion of the many connections to previous analyses for homoscedastic noise, and [11, Section S1] for a detailed discussion of connections to spiked covariance models.

Recent work [29] considers noise that is heteroscedastic within each sample, producing a non-uniform bias along the diagonal of the covariance matrix that skews its eigenvectors. To address this issue, they propose an algorithm called HeteroPCA that iteratively replaces the diagonal entries with those of the current estimate’s low-rank approximation, and they show that it has minimax optimal rate for recovering the principal subspace. Dobriban, Leeb and Singer [8] also study a data model with noise heteroscedasticity within samples, but with the goal of optimally shrinking singular values to recover low-rank signals from linearly transformed data. In contrast to both these works, we seek to optimally weight samples in PCA to address noise with across-sample heteroscedasticity. Understanding if and how these various questions and techniques relate is an interesting area for future investigation.

1.5. *Organization of the paper.* Section 2 describes the model we consider for underlying components in heteroscedastic noise, and Section 3 states the main analysis result (Theorem 1): expressions for asymptotic WPCA recovery. Section 4 outlines its proof. Section 5 derives optimal weights for component recovery (Theorem 6), and Section 6 discusses the suboptimality, or in some cases, the near optimality, of other choices. Section 7 illustrates the ways weighting affects how recovery depends on the data parameters. Section 8 derives optimal sampling strategies under budget constraints (Theorem 7). Section 9 illustrates in simulation how the asymptotic predictions compare to the empirical performance of WPCA for various problem sizes. The appendix contains the detailed proofs, and code for reproducing the figures in this paper can be found online at: <https://gitlab.com/dahong/optimally-weighted-pca-heteroscedastic-data>

2. Model for heteroscedastic data. We model n sample vectors $y_1, \dots, y_n \in \mathbb{C}^d$ as

$$(3) \quad y_j = \underbrace{\sum_{i=1}^k u_i \theta_i (z_i^{(j)})^*}_{x_j \in \mathbb{C}^d} + \eta_j \varepsilon_j = x_j + \eta_j \varepsilon_j.$$

The following are deterministic:

- $u_1, \dots, u_k \in \mathbb{C}^d$ are orthonormal components,
- $\theta_1, \dots, \theta_k > 0$ are amplitudes,
- $\eta_j \in \{\sigma_1, \dots, \sigma_L\}$ are each one of L noise standard deviations $\sigma_1, \dots, \sigma_L$,

and we define n_1 to be the number of samples with $\eta_j = \sigma_1$, n_2 to be the number of samples with $\eta_j = \sigma_2$, and so on, where $n_1 + \dots + n_L = n$.

The following are random:

- $z_1, \dots, z_k \in \mathbb{C}^n$ are iid score vectors whose entries are iid with mean $\mathbb{E}(z_i^{(j)}) = 0$, variance $\mathbb{E}|z_i^{(j)}|^2 = 1$, and a distribution satisfying a log-Sobolev inequality [1, Section 2.3.2],
- $\varepsilon_j \in \mathbb{C}^d$ are unitarily invariant iid noise vectors that have iid entries with mean $\mathbb{E}(\varepsilon_j^{(s)}) = 0$, variance $\mathbb{E}|\varepsilon_j^{(s)}|^2 = 1$ and bounded fourth moment $\mathbb{E}|\varepsilon_j^{(s)}|^4 < \infty$.

In words, (3) models data samples as containing k underlying components with additive mean zero heteroscedastic noise. Without loss of generality, we further assume that the weights correspond to the noise variances, that is, samples with noise variance $\eta_j^2 = \sigma_1^2$ are weighted as $\omega_j^2 = w_1^2$, and so on.

REMARK 1 (Unitary invariance). *Unitarily invariant noise means that left multiplication of each noise vector ε_j by any unitary matrix does not affect the joint distribution of its entries. As in our previous work [11, Remarks 1], this assumption can be removed if the set of components u_1, \dots, u_k is isotropically drawn at random as in [4, Section 2.1].*

REMARK 2 (Example distributions). *The conditions above are all satisfied when the entries $z_i^{(j)}$ and $\varepsilon_j^{(s)}$ are, for example, circularly symmetric complex normal $\mathcal{CN}(0, 1)$ or real-valued normal $\mathcal{N}(0, 1)$. Rademacher random variables (i.e., ± 1 with equal probability) are another choice for scores $z_i^{(j)}$. We are unaware of non-Gaussian distributions satisfying all the noise conditions, but as noted in Remark 1, unitary invariance can be removed if the components are random.*

3. Asymptotic performance of weighted PCA. The following theorem quantifies how well the weighted PCA estimates $\hat{u}_1, \dots, \hat{u}_k, \hat{\theta}_1, \dots, \hat{\theta}_k$, and $\hat{z}_1, \dots, \hat{z}_k$ recover the underlying components u_1, \dots, u_k , amplitudes $\theta_1, \dots, \theta_k$, and scores z_1, \dots, z_k , from (3) as a function of:

- limiting sample-to-dimension ratio $n/d \rightarrow c > 0$,
- underlying amplitudes $\theta_1, \dots, \theta_k$,
- noise variances $\sigma_1^2, \dots, \sigma_L^2$,
- weights w_1^2, \dots, w_L^2 , and
- limiting proportions $n_1/n \rightarrow p_1, \dots, n_L/n \rightarrow p_L$.

The expressions enable us to later study the behavior of weighted PCA and to optimize the weights.

THEOREM 1 (Asymptotic recovery of amplitudes, components, and scores). *Suppose the sample-to-dimension ratio $n/d \rightarrow c > 0$ and the noise variance proportions $n_\ell/n \rightarrow p_\ell$ for $\ell = 1, \dots, L$ as $n, d \rightarrow \infty$. Then the i th WPCA amplitude $\hat{\theta}_i$ converges as*

$$(4) \quad \hat{\theta}_i^2 \xrightarrow{\text{a.s.}} \frac{1}{c} \max(\alpha, \beta_i) C(\max(\alpha, \beta_i)) =: r_i^{(\theta)},$$

where α and β_i are, respectively, the largest real roots of

$$(5) \quad A(x) := 1 - c \sum_{\ell=1}^L \frac{p_\ell w_\ell^4 \sigma_\ell^4}{(x - w_\ell^2 \sigma_\ell^2)^2}, \quad B_i(x) := 1 - c \theta_i^2 \sum_{\ell=1}^L \frac{p_\ell w_\ell^2}{x - w_\ell^2 \sigma_\ell^2},$$

and where

$$(6) \quad C(x) := 1 + c \sum_{\ell=1}^L \frac{p_\ell w_\ell^2 \sigma_\ell^2}{x - w_\ell^2 \sigma_\ell^2}.$$

Furthermore, if $A(\beta_i) > 0$ then the i th component \hat{u}_i has asymptotic recovery

$$(7) \quad \sum_{j:\theta_j=\theta_i} |\langle \hat{u}_i, u_j \rangle|^2 \xrightarrow{\text{a.s.}} \frac{1}{\beta_i} \frac{A(\beta_i)}{B_i'(\beta_i)} =: r_i^{(u)}, \quad \sum_{j:\theta_j \neq \theta_i} |\langle \hat{u}_i, u_j \rangle|^2 \xrightarrow{\text{a.s.}} 0,$$

the normalized i th score \hat{z}_i/\sqrt{n} has asymptotic weighted recovery

$$(8) \quad \sum_{j:\theta_j=\theta_i} \left| \left\langle \frac{\hat{z}_i}{\sqrt{n}}, \frac{z_j}{\sqrt{n}} \right\rangle_{\mathbf{W}^2} \right|^2 \xrightarrow{\text{a.s.}} \frac{1}{c \theta_i^2 C(\beta_i)} \frac{A(\beta_i)}{B_i'(\beta_i)} =: r_i^{(z)},$$

$$\sum_{j:\theta_j \neq \theta_i} \left| \left\langle \frac{\hat{z}_i}{\sqrt{n}}, \frac{z_j}{\sqrt{n}} \right\rangle_{\mathbf{W}^2} \right|^2 \xrightarrow{\text{a.s.}} 0,$$

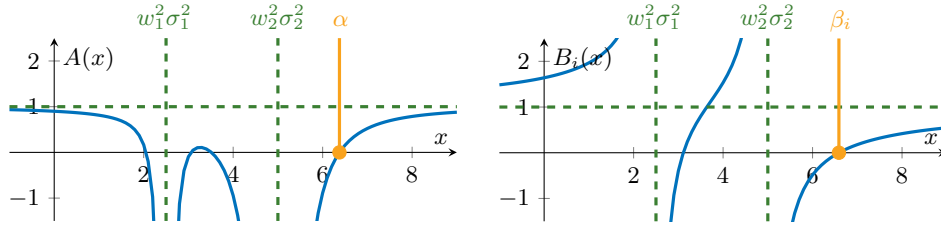


FIG 1. Location of the largest real roots α and β_i of A and B_i , respectively, for $c = 0.1$ samples per dimension, underlying amplitude $\theta_i^2 = 16$, $p_1 = 25\%$ of samples having noise variance $\sigma_1^2 = 1$ and weight $w_1^2 = 2.5$, and $p_2 = 75\%$ of samples having noise variance $\sigma_2^2 = 5$ and weight $w_2^2 = 1$.

and

$$(9) \quad \sum_{j:\theta_j=\theta_i} \langle \hat{u}_i, u_j \rangle \left\langle \frac{\hat{z}_i}{\sqrt{n}}, \frac{z_j}{\sqrt{n}} \right\rangle_{\mathbf{W}^2}^* \xrightarrow{\text{a.s.}} \sqrt{r_i^{(u)} r_i^{(z)}} = \frac{1}{\sqrt{c\theta_i^2 \beta_i C(\beta_i)}} \frac{A(\beta_i)}{B_i'(\beta_i)}.$$

Section 4 outlines the proof of Theorem 1 with the details deferred to Appendix A. An overall roadmap is as follows: a) analyze almost sure limits of two key normalized traces, b) extend [4, Theorems 2.9-2.10] using these limits to account for weighting, then c) simplify the resulting expressions. Among other challenges, the fact that weights are associated with specific samples complicates the analysis.

REMARK 3 (Location of the largest real roots). *Finding the largest real roots of the univariate rational functions $A(x)$ and $B_i(x)$ is the most challenging aspect of computing the expressions in Theorem 1, but they can be found efficiently, e.g., with bisection, by observing that they are the only roots larger than the largest pole $\max_\ell(w_\ell^2 \sigma_\ell^2)$ as shown in Fig. 1.*

REMARK 4 (Scaling properties for the weights). *Scaling all the weights w_1^2, \dots, w_L^2 does not affect the relative influence given to samples, and as a result, doing so only scales the WPCA amplitudes and scores. Theorem 1 reflects this scaling property of WPCA. Scaling all the weights by a constant λ , scales β_i by λ . As a result, $A(\beta_i)$ and $C(\beta_i)$ are unchanged, and $B_i'(\beta_i)$ is scaled by $1/\lambda$. Thus, as expected, the asymptotic component recovery (7) is unchanged, and the asymptotic amplitude (4) and asymptotic weighted score recovery (8) are both scaled by λ .*

3.1. *Special cases: uniform, binary, and inverse noise variance weights.* Uniform weights $w_\ell^2 = 1$ correspond to unweighted PCA, and binary weights

$w_\ell^2 \in \{0, 1\}$ correspond to unweighted PCA carried out on only samples with nonzero weight. As a result, the analysis of unweighted PCA in [11, Section 2] applies to uniform and binary weights. Theorem 1 specializes exactly to [11, Theorem 1] for these weights. As shown in [11, Section 2.6], the performance with these weights degrades (for both fixed average noise variance and for fixed average inverse noise variance) when the noise is heteroscedastic among the samples used. Binary weights can be chosen to use only samples with the same noise variance but doing so would preclude using all the data. Further discussion of the resulting tradeoff is in [11, Section 3.4] and Section 7.4.

Inverse noise variance weights $w_\ell^2 = 1/\sigma_\ell^2$ do not correspond to an unweighted PCA and were not analyzed in [11]. The following corollary uses Theorem 1 to provide new simple expressions for these weights.

COROLLARY 2 (Asymptotic recoveries for inverse noise variance weights). *Suppose the sample-to-dimension ratio $n/d \rightarrow c > 0$ and the noise variance proportions $n_\ell/n \rightarrow p_\ell$ for $\ell = 1, \dots, L$ as $n, d \rightarrow \infty$, and let the weights be set as $w_\ell^2 = \bar{\sigma}^2/\sigma_\ell^2$ where $\bar{\sigma}^{-2} := p_1/\sigma_1^2 + \dots + p_L/\sigma_L^2$ is the average inverse noise variance. Then the i th WPCA amplitude $\hat{\theta}_i$ converges as*

$$(10) \quad \hat{\theta}_i^2 \xrightarrow{\text{a.s.}} r_i^{(\theta)} = \begin{cases} \theta_i^2 \{1 + \bar{\sigma}^2/(c\theta_i^2)\} (1 + \bar{\sigma}^2/\theta_i^2) & \text{if } c\theta_i^4 > \bar{\sigma}^4, \\ \bar{\sigma}^2 (1 + 1/\sqrt{c})^2 & \text{otherwise.} \end{cases}$$

Furthermore, if $c\theta_i^4 > \bar{\sigma}^4$ then the i th component \hat{u}_i has asymptotic recovery

$$(11) \quad \sum_{j:\theta_j=\theta_i} |\langle \hat{u}_i, u_j \rangle|^2 \xrightarrow{\text{a.s.}} r_i^{(u)} = \frac{c - \bar{\sigma}^4/\theta_i^4}{c + \bar{\sigma}^2/\theta_i^2}, \quad \sum_{j:\theta_j \neq \theta_i} |\langle \hat{u}_i, u_j \rangle|^2 \xrightarrow{\text{a.s.}} 0,$$

and the normalized i th score \hat{z}_i/\sqrt{n} has asymptotic weighted recovery

$$(12) \quad \sum_{j:\theta_j=\theta_i} \left| \left\langle \frac{\hat{z}_i}{\sqrt{n}}, \frac{z_j}{\sqrt{n}} \right\rangle_{\mathbf{W}^2} \right|^2 \xrightarrow{\text{a.s.}} r_i^{(z)} = \frac{c - \bar{\sigma}^4/\theta_i^4}{c(1 + \bar{\sigma}^2/\theta_i^2)},$$

$$\sum_{j:\theta_j \neq \theta_i} \left| \left\langle \frac{\hat{z}_i}{\sqrt{n}}, \frac{z_j}{\sqrt{n}} \right\rangle_{\mathbf{W}^2} \right|^2 \xrightarrow{\text{a.s.}} 0.$$

PROOF OF COROLLARY 2. When $w_\ell^2 = \bar{\sigma}^2/\sigma_\ell^2$, (5) and (6) simplify to

$$A(x) = 1 - \frac{c\bar{\sigma}^4}{(x - \bar{\sigma}^2)^2}, \quad B_i(x) = 1 - \frac{c\theta_i^2}{x - \bar{\sigma}^2}, \quad C(x) = 1 + \frac{c\bar{\sigma}^2}{x - \bar{\sigma}^2},$$

yielding $\alpha = \bar{\sigma}^2(1 + \sqrt{c})$ and $\beta_i = \bar{\sigma}^2 + c\theta_i^2$. Substituting into (4), (7) and (8) in Theorem 1 yields (10)–(12). \square

Observe that $\bar{\sigma}^2$ captures the overall noise level, and performance with inverse noise variance weights is the same as that for homoscedastic noise of variance $\bar{\sigma}^2$. In contrast to uniform and binary weights, the performance of inverse noise variance weights for fixed average inverse noise variance does not degrade with heteroscedasticity because the weights always whiten the noise to be homoscedastic. In fact, performance for fixed average noise variance improves with heteroscedasticity, with perfect recovery occurring when one noise variance is taken to zero with the rest set to have the desired average. As we show in Section 5, however, these weights generally result in suboptimal asymptotic component recovery (7).

3.2. Aggregate performance of weighted PCA. The following corollary applies Theorem 1 to analyze aggregate recovery of the components, scores and samples.

COROLLARY 3 (Aggregate recovery). *Suppose the conditions of Theorem 1 hold, and additionally $A(\beta_1), \dots, A(\beta_k) > 0$. Then the WPCA component subspace basis $\hat{\mathbf{U}} := (\hat{u}_1, \dots, \hat{u}_k) \in \mathbb{C}^{d \times k}$ recovers the underlying subspace basis $\mathbf{U} := (u_1, \dots, u_k) \in \mathbb{C}^{d \times k}$ asymptotically as*

$$(13) \quad \|\hat{\mathbf{U}}^H \mathbf{U}\|_F^2 \xrightarrow{\text{a.s.}} \sum_{i=1}^k r_i^{(u)} = \sum_{i=1}^k \frac{1}{\beta_i} \frac{A(\beta_i)}{B'_i(\beta_i)},$$

the aggregate WPCA scores $\hat{\mathbf{Z}} := (\hat{z}_1, \dots, \hat{z}_k) \in \mathbb{C}^{n \times k}$ recover their underlying counterparts $\mathbf{Z} := (z_1, \dots, z_k) \in \mathbb{C}^{n \times k}$ asymptotically as

$$(14) \quad \frac{1}{n^2} \|\hat{\mathbf{Z}}^H \mathbf{W}^2 \mathbf{Z}\|_F^2 \xrightarrow{\text{a.s.}} \sum_{i=1}^k r_i^{(z)} = \sum_{i=1}^k \frac{1}{c\theta_i^2 C(\beta_i)} \frac{A(\beta_i)}{B'_i(\beta_i)},$$

and the reconstructed samples $\hat{x}_1, \dots, \hat{x}_n$ have asymptotic (weighted) mean square error with respect to the underlying samples x_1, \dots, x_n given by

$$(15) \quad \frac{1}{n} \sum_{j=1}^n \omega_j^2 \|\hat{x}_j - x_j\|_2^2 \xrightarrow{\text{a.s.}} \frac{1}{c} \sum_{i=1}^k \left\{ c\bar{w}^2 \theta_i^2 + \beta_i C(\beta_i) - 2 \frac{A(\beta_i)}{B'_i(\beta_i)} \right\},$$

where $\bar{w}^2 := p_1 w_1^2 + \dots + p_L w_L^2$.

PROOF OF COROLLARY 3. The subspace and aggregate score recoveries

decompose as

$$(16) \quad \|\hat{\mathbf{U}}^H \mathbf{U}\|_F^2 = \sum_{i=1}^k \left(\sum_{j:\theta_j=\theta_i} |\langle \hat{u}_i, u_j \rangle|^2 + \sum_{j:\theta_j \neq \theta_i} |\langle \hat{u}_i, u_j \rangle|^2 \right),$$

$$(17) \quad \frac{1}{n^2} \|\hat{\mathbf{Z}}^H \mathbf{W}^2 \mathbf{Z}\|_F^2 = \sum_{i=1}^k \left(\sum_{j:\theta_j=\theta_i} \left| \left\langle \frac{\hat{z}_i}{\sqrt{n}}, \frac{z_j}{\sqrt{n}} \right\rangle_{\mathbf{W}^2} \right|^2 + \sum_{j:\theta_j \neq \theta_i} \left| \left\langle \frac{\hat{z}_i}{\sqrt{n}}, \frac{z_j}{\sqrt{n}} \right\rangle_{\mathbf{W}^2} \right|^2 \right).$$

Substituting (7)–(8) into (16)–(17) yields (13)–(14).

The (weighted) mean square error decomposes as

$$(18) \quad \frac{1}{n} \sum_{j=1}^n \omega_j^2 \|\hat{x}_j - x_j\|_2^2 = \left\| \hat{\mathbf{U}} \hat{\mathbf{\Theta}} \left(\frac{1}{\sqrt{n}} \hat{\mathbf{Z}} \right)^H \mathbf{W} - \mathbf{U} \mathbf{\Theta} \left(\frac{1}{\sqrt{n}} \mathbf{Z} \right)^H \mathbf{W} \right\|_F^2 \\ = \sum_{i=1}^k \hat{\theta}_i^2 + \frac{\theta_i^2}{n} \|\mathbf{W} z_i\|_2^2 - 2\Re \left(\hat{\theta}_i \sum_{j=1}^k \theta_j \langle \hat{u}_i, u_j \rangle \left\langle \frac{\hat{z}_i}{\sqrt{n}}, \frac{z_j}{\sqrt{n}} \right\rangle_{\mathbf{W}^2}^* \right)$$

where $\hat{\mathbf{\Theta}} := \text{diag}(\hat{\theta}_1, \dots, \hat{\theta}_k) \in \mathbb{R}^{k \times k}$ and $\mathbf{\Theta} := \text{diag}(\theta_1, \dots, \theta_k) \in \mathbb{R}^{k \times k}$ are diagonal matrices of amplitudes, and \Re denotes the real part of its argument. The first term of (18) has almost sure limit given by (4), and the second term has almost sure limit $\theta_i^2(p_1 w_1^2 + \dots + p_L w_L^2)$ by the law of large numbers. The inner sum of the third term simplifies since summands with $\theta_j \neq \theta_i$ are zero by (7)–(8); the remaining sum has almost sure limit given by (9). Substituting the almost sure limits and simplifying yields (15). \square

3.3. Conjectured phase transition. The expressions for asymptotic component recovery (7) and asymptotic score recovery (8) in Theorem 1 and the resulting recoveries in Corollary 3 apply only when $A(\beta_i) > 0$. The following conjecture predicts a phase transition when $A(\beta_i) = 0$ resulting in zero asymptotic recovery when $A(\beta_i) \leq 0$.

CONJECTURE 4 (Phase transition). *Suppose the sample-to-dimension ratio $n/d \rightarrow c > 0$ and the noise variance proportions $n_\ell/n \rightarrow p_\ell$ for $\ell = 1, \dots, L$ as $n, d \rightarrow \infty$. If $A(\beta_i) \leq 0$ then*

$$(19) \quad \sum_{j=1}^k |\langle \hat{u}_i, u_j \rangle|^2 \xrightarrow{\text{a.s.}} 0, \quad \sum_{j=1}^k \left| \left\langle \frac{\hat{z}_i}{\sqrt{n}}, \frac{z_j}{\sqrt{n}} \right\rangle_{\mathbf{W}^2} \right|^2 \xrightarrow{\text{a.s.}} 0.$$

Namely, (7) and (8) extend to $A(\beta_i) \leq 0$ by truncating $r_i^{(u)}$ and $r_i^{(z)}$ at zero.

4. Proof sketch for Theorem 1. This section provides a rough outline, deferring the details to Appendix A. Observe first that in matrix form, the model (3) for the data matrix $\mathbf{Y} := (y_1, \dots, y_n) \in \mathbb{C}^{d \times n}$ is

$$(20) \quad \mathbf{Y} = \underbrace{(u_1, \dots, u_k)}_{\mathbf{U} \in \mathbb{C}^{d \times k}} \underbrace{\text{diag}(\theta_1, \dots, \theta_k)}_{\mathbf{\Theta} \in \mathbb{R}^{k \times k}} \underbrace{(z_1, \dots, z_k)^{\text{H}}}_{\mathbf{Z} \in \mathbb{R}^{n \times k}} + \underbrace{(\varepsilon_1, \dots, \varepsilon_n)}_{\mathbf{E} \in \mathbb{C}^{d \times n}} \underbrace{\text{diag}(\eta_1, \dots, \eta_n)}_{\mathbf{H} \in \mathbb{C}^{n \times n}}.$$

The weighted PCA components $\hat{u}_1, \dots, \hat{u}_k$, amplitudes $\hat{\theta}_1, \dots, \hat{\theta}_k$, and normalized weighted scores $\mathbf{W}\hat{z}_1/\sqrt{n}, \dots, \mathbf{W}\hat{z}_k/\sqrt{n}$ are, respectively, principal left singular vectors, singular values, and right singular vectors of the normalized and weighted data matrix

$$(21) \quad \tilde{\mathbf{Y}} := \frac{1}{\sqrt{n}} \mathbf{Y} \underbrace{\text{diag}(\omega_1^2, \dots, \omega_n^2)}_{\mathbf{W} \in \mathbb{R}^{n \times n}} = \mathbf{U} \mathbf{\Theta} \tilde{\mathbf{Z}}^{\text{H}} \mathbf{W} + \tilde{\mathbf{E}},$$

where $\tilde{\mathbf{Z}} := \mathbf{Z}/\sqrt{n}$ are normalized underlying scores and $\tilde{\mathbf{E}} := \mathbf{E}\mathbf{H}\mathbf{W}/\sqrt{n}$ are normalized and weighted noise. Namely, $\tilde{\mathbf{Y}}$ is a low-rank perturbation of a random matrix. We extend [4, Theorems 2.9-2.10] to account for weights, then exploit structure in the expressions similar to [11, Theorem 1].

As shown in [3, Chapters 4, 6] and discussed in [11, Section 5.1], the singular value distribution of $\tilde{\mathbf{E}}$ converges almost surely weakly to a nonrandom compactly supported measure $\mu_{\tilde{\mathbf{E}}}$, and the largest singular value of $\tilde{\mathbf{E}}$ converges almost surely to the supremum b of the support of $\mu_{\tilde{\mathbf{E}}}$. Hence, as reviewed in Appendix A.1,

$$(22) \quad \frac{1}{d} \text{tr} \zeta (\zeta^2 \mathbf{I} - \tilde{\mathbf{E}} \tilde{\mathbf{E}}^{\text{H}})^{-1} \xrightarrow{\text{a.s.}} \varphi_1(\zeta) := \int \frac{\zeta}{\zeta^2 - t^2} d\mu_{\tilde{\mathbf{E}}}(t),$$

where the convergence is uniform on $\{\zeta \in \mathbb{C} : \Re(\zeta) > b + \tau\}$ for any $\tau > 0$, and φ_1 has the following properties:

$$(23) \quad \forall \zeta > b \quad \varphi_1(\zeta) > 0, \quad \varphi_1(\zeta) \rightarrow 0 \text{ as } |\zeta| \rightarrow \infty, \quad \varphi_1(\zeta) \in \mathbb{R} \Leftrightarrow \zeta \in \mathbb{R}.$$

Furthermore, for any $\zeta \in \mathbb{C}$ with $\Re(\zeta) > b$,

$$(24) \quad \frac{\partial}{\partial \zeta} \frac{1}{d} \text{tr} \zeta (\zeta^2 \mathbf{I} - \tilde{\mathbf{E}} \tilde{\mathbf{E}}^{\text{H}})^{-1} \xrightarrow{\text{a.s.}} \varphi_1'(\zeta).$$

The main technical challenge in extending [4, Theorems 2.9-2.10] to account for the weights lies in proving analogous weighted results stated in the following lemma.

LEMMA 5. *Under the model assumptions in Section 2,*

$$(25) \quad \frac{1}{n} \operatorname{tr} \zeta \mathbf{W} (\zeta^2 \mathbf{I} - \tilde{\mathbf{E}}^H \tilde{\mathbf{E}})^{-1} \mathbf{W} \xrightarrow{\text{a.s.}} \varphi_2(\zeta) := \sum_{\ell=1}^L \frac{p_\ell w_\ell^2}{\zeta - w_\ell^2 \sigma_\ell^2 \varphi_1(\zeta)/c},$$

where the convergence is uniform on $\{\zeta \in \mathbb{C} : \Re(\zeta) > b + \tau\}$ for any $\tau > 0$, and φ_2 has the following properties:

$$(26) \quad \forall_{\zeta > b} \varphi_2(\zeta) > 0, \quad \varphi_2(\zeta) \rightarrow 0 \text{ as } |\zeta| \rightarrow \infty, \quad \varphi_2(\zeta) \in \mathbb{R} \Leftrightarrow \zeta \in \mathbb{R}.$$

Furthermore, for any $\zeta \in \mathbb{C}$ with $\Re(\zeta) > b$,

$$(27) \quad \frac{\partial}{\partial \zeta} \frac{1}{n} \operatorname{tr} \zeta \mathbf{W} (\zeta^2 \mathbf{I} - \tilde{\mathbf{E}}^H \tilde{\mathbf{E}})^{-1} \mathbf{W} \xrightarrow{\text{a.s.}} \varphi_2'(\zeta).$$

Lemma 5 is proved in Appendix B and enables us to extend [4, Theorems 2.9-2.10] in Appendices A.2 and A.3 to conclude that for each $i \in \{1, \dots, k\}$,

$$(28) \quad \hat{\theta}_i^2 \xrightarrow{\text{a.s.}} \begin{cases} \rho_i^2 & \text{if } \theta_i^2 > \bar{\theta}^2, \\ b^2 & \text{otherwise,} \end{cases} =: r_i^{(\theta)}$$

and when $\theta_i^2 > \bar{\theta}^2$,

$$(29) \quad \sum_{j:\theta_j=\theta_i} |\langle \hat{u}_i, u_j \rangle|^2 \xrightarrow{\text{a.s.}} \frac{-2\varphi_1(\rho_i)}{\theta_i^2 D'(\rho_i)} =: r_i^{(u)},$$

$$(30) \quad \sum_{j:\theta_j=\theta_i} \left| \left\langle \frac{\hat{z}_i}{\sqrt{n}}, \frac{z_j}{\sqrt{n}} \right\rangle_{\mathbf{W}^2} \right|^2 \xrightarrow{\text{a.s.}} \frac{-2\varphi_2(\rho_i)}{\theta_i^2 D'(\rho_i)} =: r_i^{(z)},$$

$$(31) \quad \sum_{j:\theta_j \neq \theta_i} |\langle \hat{u}_i, u_j \rangle|^2, \quad \sum_{j:\theta_j \neq \theta_i} \left| \left\langle \frac{\hat{z}_i}{\sqrt{n}}, \frac{z_j}{\sqrt{n}} \right\rangle_{\mathbf{W}^2} \right|^2 \xrightarrow{\text{a.s.}} 0,$$

and

$$(32) \quad \sum_{j:\theta_j=\theta_i} \langle \hat{u}_i, u_j \rangle \left\langle \frac{\hat{z}_i}{\sqrt{n}}, \frac{z_j}{\sqrt{n}} \right\rangle_{\mathbf{W}^2}^* \xrightarrow{\text{a.s.}} \sqrt{r_i^{(u)} r_i^{(z)}},$$

where $D(\zeta) := \varphi_1(\zeta)\varphi_2(\zeta)$, $\rho_i := D^{-1}(1/\theta_i^2)$ and $\bar{\theta}^2 := 1/\lim_{\zeta \rightarrow b^+} D(\zeta)$.

The final step (Appendix A.4) is to find algebraic descriptions of $r_i^{(u)}$ and $r_i^{(z)}$. We change variables to $\psi(\zeta) := c\zeta/\varphi_1(\zeta)$ and, analogous to [11, Section 5.3], observe that ψ has the following properties:

a) $0 = Q(\psi(\zeta), \zeta)$ for all $\zeta > b$ where

$$(33) \quad Q(s, \zeta) := \frac{c\zeta^2}{s^2} + \frac{c-1}{s} - c \sum_{\ell=1}^L \frac{p_\ell}{s - w_\ell^2 \sigma_\ell^2},$$

with the inverse function given by

$$(34) \quad \psi^{-1}(\gamma) = \sqrt{\frac{\gamma}{c} \left(1 + c \sum_{\ell=1}^L \frac{p_\ell w_\ell^2 \sigma_\ell^2}{\gamma - w_\ell^2 \sigma_\ell^2} \right)},$$

b) $\max_\ell(\sigma_\ell^2 w_\ell^2) < \psi(\zeta) < c\zeta^2$,

c) $0 < \lim_{\zeta \rightarrow b^+} \psi(\zeta) < \infty$ and $\lim_{\zeta \rightarrow b^+} \psi'(\zeta) = \infty$.

Combining these properties with the observation that

$$(35) \quad D(\zeta) = \varphi_1(\zeta) \sum_{\ell=1}^L \frac{p_\ell w_\ell^2}{z - w_\ell^2 \sigma_\ell^2 \varphi_1(\zeta)/c} = c \sum_{\ell=1}^L \frac{p_\ell w_\ell^2}{\psi(\zeta) - w_\ell^2 \sigma_\ell^2},$$

then simplifying analogously to [11, Sections 5.4–5.6], yields (4)–(9) and concludes the proof.

5. Optimally weighted PCA. The following theorem optimizes the expressions in Theorem 1 to find weights that maximize component recovery.

THEOREM 6 (Optimal component recovery). *The weights*

$$(36) \quad w_\ell^2 = \frac{1}{\sigma_\ell^2} \frac{1}{\theta_i^2 + \sigma_\ell^2},$$

maximize the asymptotic recovery $r_i^{(u)}$ of the i th underlying component u_i by the WPCA component \hat{u}_i with the corresponding optimal value of $r_i^{(u)}$ given by the largest real root of

$$(37) \quad R_i^{(u)}(x) := 1 - c\theta_i^2 \sum_{\ell=1}^L \frac{p_\ell}{\sigma_\ell^2} \frac{1-x}{\sigma_\ell^2/\theta_i^2 + x}.$$

When $\theta_i^2 \gg \sigma_1^2, \dots, \sigma_L^2$, i.e., when the noise is relatively small, $1/(\theta_i^2 + \sigma_\ell^2)$ becomes uniform over ℓ and the optimal weights (36) reduce to inverse noise variance weights, providing further justification for these commonly used weights. However, when $\theta_i^2 \ll \sigma_1^2, \dots, \sigma_L^2$ and the noise is relatively large, $1/(\theta_i^2 + \sigma_\ell^2)$ becomes $1/\sigma_\ell^2$ and the optimal weights reduce to *square* inverse

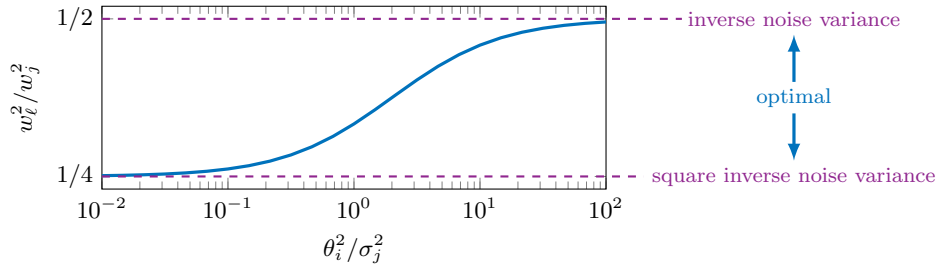


FIG 2. Relative weight w_ℓ^2/w_j^2 given by optimal weights (36) to samples with twice the noise variance $\sigma_\ell^2 = 2\sigma_j^2$ as a function of the underlying amplitude θ_i^2 . As the underlying amplitude increases, optimal weighting interpolates between square inverse noise variance weights ($w_\ell^2/w_j^2 = 1/4$) and inverse noise variance weights ($w_\ell^2/w_j^2 = 1/2$).

noise variance weights. Inverse noise variance weights do not downweight noisier samples aggressively enough when the signal-to-noise ratio is small. Rather than give samples with twice the noise variance half the weight as with inverse noise variance weights, it is better to give them a quarter the weight in this regime. In general, optimal weights strike a balance between inverse noise variance weights and square inverse noise variance weights, as

$$\frac{1/\sigma_\ell^4}{1/\sigma_j^4} < \frac{\sigma_j^4 \theta_i^2/\sigma_j^2 + 1}{\sigma_\ell^4 \theta_i^2/\sigma_\ell^2 + 1} = \frac{w_\ell^2}{w_j^2} = \frac{\sigma_j^2 \theta_i^2 + \sigma_j^2}{\sigma_\ell^2 \theta_i^2 + \sigma_\ell^2} < \frac{1/\sigma_\ell^2}{1/\sigma_j^2},$$

for any two noise variances $\sigma_\ell^2 > \sigma_j^2$. Samples with twice the noise variance are given between a half and a quarter of the weight, with the particular balance dictated by the underlying amplitude θ_i^2 , as shown in Fig. 2. In practice, one may estimate the underlying amplitudes θ_i^2 by de-biasing PCA estimates $\hat{\theta}_i^2$ using expressions like (4).

Interestingly, the optimal weights (36) depend on neither the sample-to-dimension ratio c nor proportions p_1, \dots, p_L , though these properties greatly impact how informative each group of samples is on the whole, as shown in Section 6. Consequently, there is no benefit to using different weights for samples with the same noise variance. Furthermore, note that the second term $1/(\theta_i^2 + \sigma_\ell^2)$ normalizes samples by their variance in the direction of u_i .

The remainder of this section proves Theorem 6. Though the result (36) is simple to state, deriving it is nontrivial in part due to the fact that any scaling of the weights produces the same components. The proof exploits this structure to find optimal weights and their corresponding recovery.

PROOF OF THEOREM 6. The objective is to maximize $r_i^{(u)}$ with respect to the weights w_1^2, \dots, w_L^2 under the implicit constraint that the weights are

nonnegative. Partition the feasible region into $2^L - 1$ sets each defined by which weights are zero. Namely, consider partitions of the form

$$(38) \quad \mathcal{P}_{\mathcal{L}} := \{(w_1^2, \dots, w_L^2) : \forall \ell \in \mathcal{L} \ w_\ell^2 = 0, \forall \ell \notin \mathcal{L} \ w_\ell^2 > 0\},$$

where $\mathcal{L} \subset \{1, \dots, L\}$ is a proper, but potentially empty, subset. Note that the origin, where all the weights are zero, is not within the domain of $r_i^{(u)}$. Since $r_i^{(u)}$ is invariant to scaling of the weights, as discussed in Remark 4, a maximizer exists within at least one of the partitions. Moreover, since $r_i^{(u)}$ is a differentiable function of the weights, $r_i^{(u)}$ is maximized at a critical point of a partition $\mathcal{P}_{\mathcal{L}}$. It remains to identify and compare the critical points of all the partitions.

First consider \mathcal{P}_\emptyset , i.e., the set of positive weights $w_1^2, \dots, w_L^2 > 0$, and let $\tilde{w}_j := 1/w_j^2$. This reparameterization ends up simplifying the manipulations. Differentiating key terms from Theorem 1, specifically (7) and (5), with respect to \tilde{w}_j yields

$$(39) \quad \frac{\partial r_i^{(u)}}{\partial \tilde{w}_j} = r_i^{(u)} \left\{ -\frac{1}{\beta_i} \frac{\partial \beta_i}{\partial \tilde{w}_j} + \frac{1}{A(\beta_i)} \frac{\partial A(\beta_i)}{\partial \tilde{w}_j} - \frac{1}{B'_i(\beta_i)} \frac{\partial B'_i(\beta_i)}{\partial \tilde{w}_j} \right\},$$

$$(40) \quad \frac{\partial A(\beta_i)}{\partial \tilde{w}_j} = A'(\beta_i) \frac{\partial \beta_i}{\partial \tilde{w}_j} + 2c \frac{p_j \sigma_j^4}{(\beta_i \tilde{w}_j - \sigma_j^2)^3} \beta_i,$$

$$(41) \quad \frac{\partial B'_i(\beta_i)}{\partial \tilde{w}_j} = B''_i(\beta_i) \frac{\partial \beta_i}{\partial \tilde{w}_j} - 2c\theta_i^2 \frac{p_j}{(\beta_i \tilde{w}_j - \sigma_j^2)^3} \beta_i \tilde{w}_j + c\theta_i^2 \frac{p_j}{(\beta_i \tilde{w}_j - \sigma_j^2)^2},$$

$$(42) \quad 0 = \frac{\partial B_i(\beta_i)}{\partial \tilde{w}_j} = B'_i(\beta_i) \frac{\partial \beta_i}{\partial \tilde{w}_j} + c\theta_i^2 \frac{p_j}{(\beta_i \tilde{w}_j - \sigma_j^2)^2} \beta_i,$$

where one must carefully account for the fact that A and B_i are implicit functions of \tilde{w}_j , so β_i is as well. Rewriting (40) and (41) in terms of $\partial \beta_i / \partial \tilde{w}_j$ using (42) yields

$$(43) \quad \frac{\partial A(\beta_i)}{\partial \tilde{w}_j} = \left\{ A'(\beta_i) - \frac{2B'_i(\beta_i)}{\theta_i^2} \frac{\sigma_j^4}{\beta_i \tilde{w}_j - \sigma_j^2} \right\} \frac{\partial \beta_i}{\partial \tilde{w}_j},$$

$$(44) \quad \frac{\partial B'_i(\beta_i)}{\partial \tilde{w}_j} = \left\{ B''_i(\beta_i) + 2B'_i(\beta_i) \frac{\tilde{w}_j}{\beta_i \tilde{w}_j - \sigma_j^2} \right\} \frac{\partial \beta_i}{\partial \tilde{w}_j} - \frac{1}{\beta_i} B'_i(\beta_i) \frac{\partial \beta_i}{\partial \tilde{w}_j}.$$

Substituting (43) and (44) into (39) then rearranging yields

$$(45) \quad \frac{\partial r_i^{(u)}}{\partial \tilde{w}_j} = \frac{2}{\theta_i^2 \beta_i} \frac{\partial \beta_i}{\partial \tilde{w}_j} \left\{ \theta_i^2 \Delta_i - \frac{\theta_i^2 \beta_i r_i^{(u)} \tilde{w}_j + \sigma_j^4}{\beta_i \tilde{w}_j - \sigma_j^2} \right\},$$

where the following term is independent of j :

$$(46) \quad \Delta_i := \frac{1}{2} \frac{A(\beta_i)}{B'_i(\beta_i)} \left\{ \frac{A'(\beta_i)}{A(\beta_i)} - \frac{B''_i(\beta_i)}{B'_i(\beta_i)} \right\}.$$

Since $\beta_i > \max_\ell (w_\ell^2 \sigma_\ell^2) > 0$ it follows that $\partial \beta_i / \partial \tilde{w}_j \neq 0$, so (45) is zero exactly when

$$(47) \quad \theta_i^2 \Delta_i = \frac{\theta_i^2 \beta_i r_i^{(u)} \tilde{w}_j + \sigma_j^4}{\beta_i \tilde{w}_j - \sigma_j^2}.$$

Rearranging (7) and substituting (47) yields

$$(48) \quad 0 = A(\beta_i) - r_i^{(u)} \beta_i B'_i(\beta_i) = 1 - c \sum_{\ell=1}^L \frac{p_\ell (\sigma_\ell^4 + \theta_i^2 \beta_i r_i^{(u)} \tilde{w}_\ell)}{(\beta_i \tilde{w}_\ell - \sigma_\ell^2)^2}$$

$$= 1 - \Delta_i c \theta_i^2 \sum_{\ell=1}^L \frac{p_\ell}{\beta_i \tilde{w}_\ell - \sigma_\ell^2} = 1 - \Delta_i (1 - B_i(\beta_i)) = 1 - \Delta_i,$$

so $\Delta_i = 1$. Substituting into (47) and solving for \tilde{w}_j yields

$$(49) \quad w_j^2 = \frac{1}{\tilde{w}_j} = \frac{(1 - r_i^{(u)}) \theta_i^2 \beta_i}{\sigma_j^2 (\theta_i^2 + \sigma_j^2)} = \frac{\kappa_i}{\sigma_j^2 (\theta_i^2 + \sigma_j^2)},$$

where the constant $\kappa_i := (1 - r_i^{(u)}) \theta_i^2 \beta_i$ is: a) independent of j , b) parameterizes the ray of critical points in \mathcal{P}_\emptyset , and c) can be chosen freely, e.g., as unity yielding (36). Solving (49) for $\beta_i \tilde{w}_j$, substituting into (5), and rearranging yields that the corresponding $r_i^{(u)}$ is a root of $R_i^{(u)}$ in (37). Since $R_i^{(u)}(x)$ increases from negative infinity to one as x increases from $-\min_\ell (\sigma_\ell^2) / \theta_i^2$ to one, it has exactly one real root in that domain. In particular, this root is the largest real root since $R_i^{(u)}(x) \geq 1$ for $x \geq 1$. Furthermore, $r_i^{(u)}$ increases continuously to one as c increases to infinity, so $r_i^{(u)}$ is the largest real root.

Likewise, the critical points of other partitions $\mathcal{P}_{\mathcal{L}}$ are given by setting the positive weights proportional to (36) with the corresponding $r_i^{(u)}$ given by the largest real root of

$$(50) \quad R_{i,\mathcal{L}}^{(u)}(x) := 1 - c \theta_i^2 \sum_{\ell \notin \mathcal{L}} \frac{p_\ell}{\sigma_\ell^2} \frac{1 - x}{\sigma_\ell^2 / \theta_i^2 + x}.$$

For $\mathcal{L}_1 \subset \mathcal{L}_2$ a proper subset, the largest real root of $R_{i,\mathcal{L}_1}^{(u)}$ is greater than that of $R_{i,\mathcal{L}_2}^{(u)}$ since $R_{i,\mathcal{L}_1}^{(u)}(x) < R_{i,\mathcal{L}_2}^{(u)}(x)$ for any $x \in (-\min_\ell (\sigma_\ell^2) / \theta_i^2, 1)$. As a result, $r_i^{(u)}$ is maximized in \mathcal{P}_\emptyset . \square

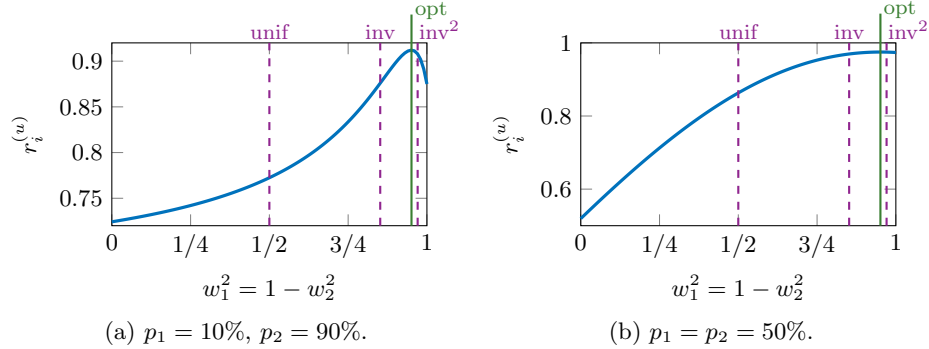


FIG 3. Asymptotic component recovery (7) for $c = 150$ samples per dimension, underlying amplitude $\theta_i^2 = 1$, and noise variances $\sigma_1^2 = 1$ and $\sigma_2^2 = 5.75$, as the weight $w_1^2 = 1 - w_2^2$ for the cleaner samples sweeps from zero to one. At the extremes only noisier samples are used ($w_1^2 = 0$) or only cleaner samples are used ($w_1^2 = 1$). Vertical lines indicate which weights correspond to unweighted PCA (unif), inverse noise variance weights (inv), square inverse noise variance weights (inv^2), and optimal weights (opt) from (36). Theorem 1 quantifies the benefit of combining in (a), and the near optimality of using only cleaner data in (b).

6. Suboptimal weighting. Theorem 1 provides a way to not only find optimal weights, but to also quantify how suboptimal other weights are. Suppose there are $c = 150$ samples per dimension, the underlying amplitude is $\theta_i^2 = 1$ and $p_1 = 10\%$ of samples have noise variance $\sigma_1^2 = 1$ with the remaining $p_2 = 90\%$ having noise variance $\sigma_2^2 = 5.75$. Figure 3a shows the asymptotic component recovery (7) as the weight w_1^2 given to the cleaner samples increases, with the weight for the noisier samples set as $w_2^2 = 1 - w_1^2$. In this case, excluding either set of samples is significantly suboptimal. Using the noisier data alone ($w_1^2 = 0$) achieves $r_i^{(u)} \approx 0.72$, using the cleaner data alone ($w_1^2 = 1$) achieves $r_i^{(u)} \approx 0.88$, and optimal weighting achieves $r_i^{(u)} \approx 0.91$. Inverse noise variance weights achieve $r_i^{(u)} \approx 0.88$ and are similar to using only the cleaner data. The optimal weights here are closer to square inverse noise variance.

Now suppose the proportions are $p_1 = p_2 = 50\%$ with all other parameters the same. Figure 3b shows the asymptotic component recovery (7). In this case, using only the cleaner data, using inverse noise variance weights, or using square inverse noise variance weights are all nearly optimal; these choices and the optimal weighting all have recovery $r_i^{(u)} \approx 0.97$. Observe that all the indicated weights are the same as those in (a) since none depend on proportions. However, the recovery depends on weights in a dramatically different way. The cleaner data is sufficiently abundant in this setting to

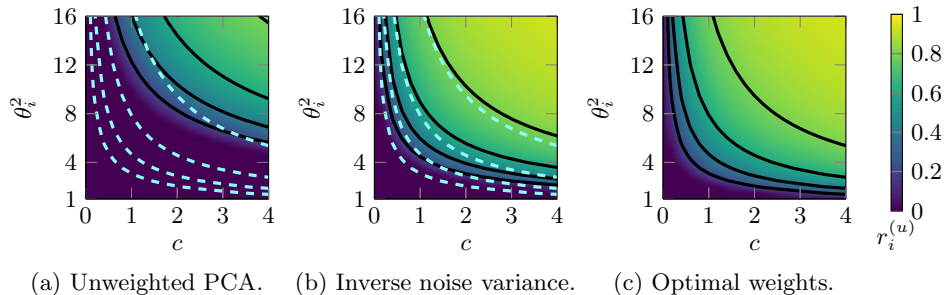


FIG 4. Asymptotic component recovery (7) as a function of the number of samples per dimension c and the underlying amplitude θ_i^2 , where $p_1 = 20\%$ of samples have noise variance $\sigma_1^2 = 1$, and the remaining $p_2 = 80\%$ have noise variance $\sigma_2^2 = 10$. Contours are shown in black, and the contours for optimal weights (c) are overlaid as light blue dashed lines in (a) and (b). Inverse noise variance and optimal weights significantly improve PCA performance, with optimal weights providing greater improvement for small amplitudes.

achieve great recovery, and the noisy data add little.

Using suboptimal weights is sometimes convenient. For example, (square) inverse noise variance weights can be applied without estimating θ_i^2 . Dropping noisier samples can reduce computational or administrative burden. For some applications, these suboptimal weights may perform sufficiently well; Theorem 1 enables quantitative reasoning about the trade-offs.

7. Impact of model parameters. Theorem 1 also provides new insight into the ways weighting changes the performance of PCA with respect to the model parameters: sample-to-dimension ratio c , amplitudes $\theta_1^2, \dots, \theta_k^2$, proportions p_1, \dots, p_L and noise variances $\sigma_1^2, \dots, \sigma_L^2$. This section compares the impact on: a) unweighted PCA, b) inverse noise variance weighted PCA, and c) optimally weighted PCA. We illustrate the phenomena with two noise variances for simplicity; the same insights apply more broadly. See also [11, Section 3] for related discussion regarding unweighted PCA.

7.1. Impact of sample-to-dimension ratio c and amplitude θ_i^2 . Suppose that $p_1 = 20\%$ of samples have noise variance $\sigma_1^2 = 1$, and the remaining $p_2 = 80\%$ have noise variance $\sigma_2^2 = 10$. Figure 4 shows the asymptotic component recovery (7) as the samples per dimension c and the underlying amplitude θ_i^2 vary. Decreasing the amplitude degrades recovery, and the lost performance can be regained by increasing the number of samples per dimension. Both inverse noise variance and optimal weights significantly outperform unweighted PCA, with optimal weights providing more improvement for small underlying amplitudes. Each contour for inverse noise vari-

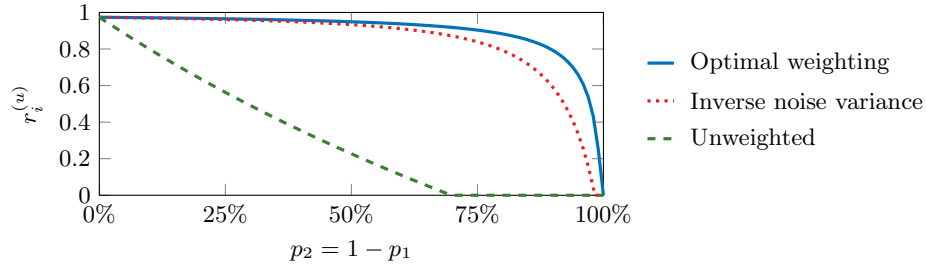


FIG 5. Asymptotic component recovery (7) as a function of the proportion p_2 of samples corrupted by noise with a large variance $\sigma_2^2 = 10$ while the remaining $p_1 = 1 - p_2$ samples have noise variance $\sigma_1^2 = 1$. There are $c = 75$ samples per dimension and the underlying amplitude is $\theta_i^2 = 1$. Inverse noise variance weighted PCA is more robust to such contaminations than unweighted PCA, and optimally weighted PCA is even more robust.

ance weights is defined by (11) in Corollary 2, and each contour for optimal weights is defined by (37) in Theorem 6.

7.2. *Impact of proportions p_1, \dots, p_L .* Suppose there are $c = 75$ samples per dimension, the underlying amplitude is $\theta_i^2 = 1$, and contaminated samples with noise variance $\sigma_2^2 = 10$ occur in proportion p_2 while the remaining $p_1 = 1 - p_2$ proportion of samples have noise variance $\sigma_1^2 = 1$. Figure 5 shows the asymptotic component recovery (7) as the contamination proportion p_2 increases. Unweighted PCA is not robust to such contamination, but inverse noise variance weights achieve good recovery for even significant amounts of contamination. Optimal weights are even more robust at extreme levels of contamination, since they more aggressively downweight noisier samples.

7.3. *Impact of noise variances $\sigma_1^2, \dots, \sigma_L^2$.* Suppose $p_1 = 70\%$ of samples have noise variance σ_1^2 , $p_2 = 30\%$ have noise variance σ_2^2 , and there are $c = 10$ samples per dimension with underlying amplitude $\theta_i^2 = 1$. Figure 6 shows the asymptotic component recovery (7) as σ_1^2 and σ_2^2 vary. In general, performance degrades as noise variances increase. As discussed in [11, Section 3.3], a large noise variance can dominate unweighted PCA performance even when it occurs in a small proportion of samples; unweighted PCA is not robust to gross errors, i.e., outliers. In Fig. 6a, the contours show that decreasing σ_1^2 does not significantly improve performance when σ_2^2 is large.

In contrast, weighted PCA performance depends more on the smallest noise variance for both inverse noise variance weights and optimal weights since both types of weights give cleaner samples more influence. In Figs. 6b and 6c, the contours show that increasing σ_1^2 does not significantly degrade performance when σ_2^2 is small and vice versa for small σ_1^2 . In particular, each

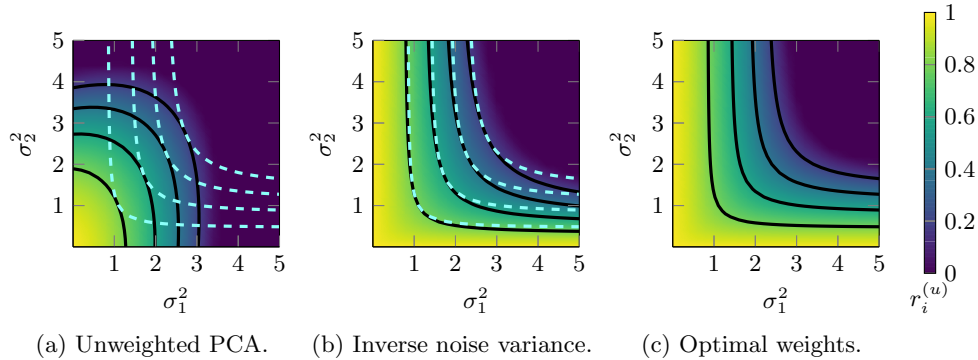


FIG 6. *Asymptotic component recovery (7) as a function of noise variances σ_1^2 and σ_2^2 appearing in proportions $p_1 = 70\%$ and $p_2 = 30\%$. There are $c = 10$ samples per dimension and the underlying amplitude is $\theta_i^2 = 1$. Contours are shown in black, and the contours for optimal weights (c) are overlaid as light blue dashed lines in (a) and (b). While unweighted PCA is most sensitive to the largest noise variance, inverse noise variance and optimal weights are most sensitive to the smallest noise variance, with optimal weights providing more improvement for large heteroscedasticity.*

contour in Fig. 6b is defined by having equal average inverse noise variance $\bar{\sigma}^{-2} := p_1/\sigma_1^2 + \dots + p_L/\sigma_L^2$; see Corollary 2. Similarly, each contour in Fig. 6c is defined by (37) in Theorem 6. In both cases, as a noise variance grows to infinity, its impact diminishes and the other noise variances determine the resulting performance. For optimal weights, this limiting performance corresponds exactly to excluding the noisiest data. Inverse noise variance weights, however, achieve worse performance in this limit as shown by the overlaid contours; excluding the noisiest data is better.

A surprising finding of [11, Section 3.3] was that adding noise sometimes improves the performance of unweighted PCA. The same is not true for inverse noise variance or optimal weights. Adding any noise increases $\bar{\sigma}^2$, degrading the performance for inverse noise variance weights. Likewise, adding noise increases the function $R_i^{(u)}$ in (37), decreasing its largest root and degrading the performance for optimal weights.

7.4. Impact of including noisier data. Consider adding c_2 samples per dimension with noise variance σ_2^2 to a dataset containing $c_1 = 10$ samples per dimension with noise variance $\sigma_1^2 = 1$, all with underlying amplitude $\theta_i^2 = 1$. The combined dataset has $c = c_1 + c_2$ samples per dimension with noise variances σ_1^2 and σ_2^2 occurring with proportions $p_1 = c_1/c$ and $p_2 = c_2/c$. Figure 7 shows the asymptotic component recovery (7) for various noise variances σ_2^2 as a function of the amount of samples c_2 . When $c_2 = 0$ only the

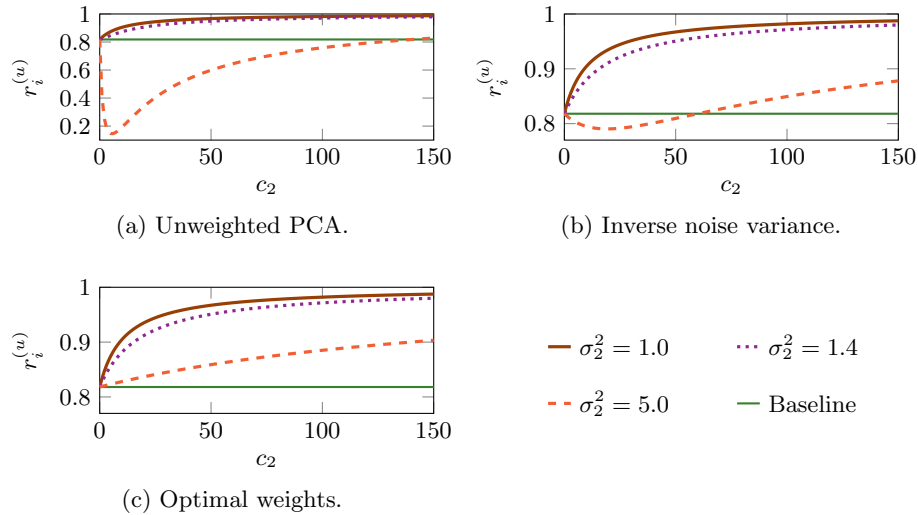


FIG 7. Asymptotic component recovery (7) as c_2 samples per dimension with noise variance σ_2^2 are added to $c_1 = 10$ samples per dimension having noise variance $\sigma_1^2 = 1$. The underlying amplitude is $\theta_i^2 = 1$. Including noisier samples can degrade the performance of unweighted PCA or inverse noise variance weights, but optimally weighted PCA always improves when given more data.

original data are used; horizontal green lines indicate this baseline recovery.

As discussed in [11, Section 3.4], the additional samples improve unweighted PCA performance when σ_2^2 is small enough or when c_2 is large enough to overcome the additional noise. Including a small number of much noisier samples degrades performance since unweighted PCA is not robust to them. Inverse noise variance weighted PCA is more robust and outperforms unweighted PCA, but including very noisy samples again degrades performance unless c_2 is large enough. Inverse noise variance weights do not downweight the noisier samples enough, and sometimes excluding noisier data is better.

With optimally weighted PCA, on the other hand, using more data always improves performance. Since the weights are optimal, they are necessarily at least as good as binary weights that exclude the noisier data. The optimal combination of original and noisier data is no worse than either one alone, so including more samples only helps. See Remark 7 for related discussion.

8. Optimal sampling under budget constraints. This section uses Theorem 6 to consider optimizing a sampling strategy to maximize the recovery of optimally weighted PCA. Specifically, consider acquiring samples

of varying quality, cost and availability under a budget. Given that the samples will be optimally weighted, what combination of inexpensive noisy samples and expensive clean samples maximizes asymptotic component recovery? What if we already have previously collected data? The following theorem uses (37) to answer these questions. Note that previously collected data are simply samples with limited availability and zero acquisition cost.

THEOREM 7 (Optimal sampling for a budget). *Consider L sources of d -dimensional samples with associated noise variances $\sigma_1^2, \dots, \sigma_L^2$ and costs τ_1, \dots, τ_L , and let $n_1, \dots, n_L \geq 0$ be the corresponding numbers of samples collected. Suppose the total cost is constrained by the available budget T as*

$$(51) \quad n_1\tau_1 + \dots + n_L\tau_L \leq T,$$

and n_1, \dots, n_L are constrained by limited availability of samples as

$$(52) \quad n_\ell \leq q_\ell, \quad \ell \in \{1, \dots, L\},$$

where q_ℓ is the quantity available for source ℓ . Then the sample-to-dimension ratios $c_1, \dots, c_L \geq 0$, defined for each $\ell \in \{1, \dots, L\}$ as $c_\ell := n_\ell/d$, are constrained to the polyhedron in the nonnegative orthant defined by

$$(53) \quad c_1\tau_1 + \dots + c_L\tau_L \leq T/d, \quad c_\ell \leq q_\ell/d, \quad \ell \in \{1, \dots, L\},$$

and the asymptotic component recovery (37) with optimal weights is maximized with respect to c_1, \dots, c_L at an extreme point of the polyhedron (53). Furthermore, all maximizers occur at points where increasing any one of c_1, \dots, c_L would violate (53), i.e., at points where the budget and availability are fully utilized.

REMARK 5 (Additional budget constraints). *Theorem 7 considers a single budget constraint (51) for simplicity, but the same result holds with multiple linear constraints. For example, one constraint may pertain to the time needed for acquiring samples and another could pertain to the money needed.*

REMARK 6 (Unlimited availability). *Theorem 7 assumes that all sources have a limited availability of samples q_ℓ for simplicity, but the same result holds as long as all sources have either nonzero cost, limited availability or both. If a source has both no cost and unlimited availability, asymptotic component recovery is maximized by acquiring increasingly many of its samples.*

REMARK 7 (Samples with no cost). *An immediate consequence of Theorem 7 is that any samples with no cost, e.g., previously collected data, should*

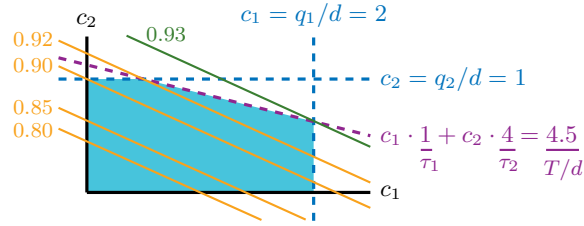


FIG 8. Optimal sampling under a budget occurs at extreme points of the polyhedron in the nonnegative orthant defined by the budget and availability constraints (53) shown in purple and blue, respectively. The total budget per dimension is $T/d = 4.5$, and samples cost $\tau_1 = 1$ and $\tau_2 = 4$ with associated availabilities per dimension $q_1/d = 2$ and $q_2/d = 1$, i.e., samples from the first source are cheaper and more abundant. Contours of $r_i^{(u)}$ for optimal weights are overlaid for noise variances $\sigma_1^2 = 2$ and $\sigma_2^2 = 1$ and an underlying amplitude $\theta_i^2 = 10$. The best contour (green) intersects the feasible polyhedron at $c_1 = 2, c_2 = 5/8$, where all available cheaper, noisier samples are collected with the remaining budget used for the higher quality samples.

always be included when using optimal weights. Doing so is, perhaps surprisingly, not always best when using unweighted or inverse noise variance weighted PCA. As demonstrated in Section 7.4, including noisier samples can degrade performance for suboptimal weights.

To illustrate Theorem 7, suppose that samples with noise variance $\sigma_1^2 = 2$ cost $\tau_1 = 1$ and have availability per dimension $q_1/d = 2$, and samples with noise variance $\sigma_2^2 = 1$ cost $\tau_2 = 4$ and have availability per dimension $q_2/d = 1$, where the overall budget per dimension is $T/d = 4.5$. Namely, the first source of samples is twice as noisy but also a quarter the cost and twice as abundant. What combination of sampling rates c_1 and c_2 maximizes recovery by optimally weighted PCA of an underlying component with associated amplitude $\theta_i^2 = 10$? As predicted by Theorem 7, the maximum in Fig. 8 occurs at an extreme point of the polyhedron in the nonnegative orthant defined by (53). Furthermore, it occurs at an extreme point where increasing either c_1 or c_2 would violate the constraints, i.e., at $c_1 = 2, c_2 = 5/8$. The other candidate extreme point is $c_1 = 1/2, c_2 = 1$, but $r_i^{(u)}$ is smaller there. In words, the optimal choice is to collect all available cheaper, noisier samples then spend the remaining budget on the more costly, higher quality samples.

The proof of Theorem 7 relies on the following lemma that generalizes the optimality of extreme points in linear programs (see, e.g., [5, Theorem 2.7]) to nonlinear objective functions for which each level set is a flat. A flat here refers to the solution set of an (underdetermined) linear system of equations, polyhedron means a finite intersection of half-spaces, and an extreme point

of a set is a point that is not a convex combination of any other points in the set; see [5, Chapter 2] for further discussion and properties. We prove Lemma 8 in Appendix C.

LEMMA 8 (Optimality of extreme points). *Let $P \subset \mathbb{R}^n$ be a polyhedron with at least one extreme point, and let $f : P \rightarrow \mathbb{R}$ be a continuous function such that each level set is a flat. If there exists a point in P that maximizes f , then there exists an extreme point of P that maximizes f .*

PROOF OF THEOREM 7. Observe first that $c = c_1 + \dots + c_L$ and $p_\ell = c_\ell/c$ for each $\ell \in \{1, \dots, L\}$, so rewriting (37) yields that $r_i^{(u)}$ is the largest real value that satisfies

$$(54) \quad 0 = R_i^{(u)}(r_i^{(u)}) = 1 - \sum_{\ell=1}^L c_\ell \frac{\theta_i^2}{\sigma_\ell^2} \frac{1 - r_i^{(u)}}{\sigma_\ell^2/\theta_i^2 + r_i^{(u)}},$$

when the weights are set optimally. Thus, $r_i^{(u)}$ is a continuous function of c_1, \dots, c_L over the domain $c_1, \dots, c_L \geq 0$ with level sets that are affine hyperplanes. The constraint set P defined by $c_1, \dots, c_L \geq 0$ and (53) is a bounded polyhedron, so contains an extreme point as well as a maximizer of $r_i^{(u)}$. Thus, Lemma 8 implies that an extreme point of P maximizes $r_i^{(u)}$.

The final statement of the theorem follows by observing that the right hand side of (54) decreases when any one of c_1, \dots, c_L increases, increasing the resulting $r_i^{(u)}$. Namely, $r_i^{(u)}$ with optimal weighting improves when any of c_1, \dots, c_L increases. As a result, any point where c_1, \dots, c_L could be increased without violating (53) cannot be a maximizer. \square

9. Numerical simulation. This section uses numerical simulations to demonstrate that the asymptotic results of Theorem 1 provide meaningful predictions for finitely many samples in finitely many dimensions. Data are generated according to the model (3) with $c = 1$ sample per dimension, underlying amplitudes $\theta_1^2 = 25$ and $\theta_2^2 = 16$, and $p_1 = 20\%$ of samples having noise variance $\sigma_1^2 = 1$ with the remaining $p_2 = 80\%$ of samples having noise variance $\sigma_2^2 = 4$. Underlying scores and unscaled noise entries are both generated from the standard normal distribution, i.e., $z_{ij}, \varepsilon_{ij} \sim \mathcal{N}(0, 1)$, and the weights are set to $w_1^2 = (1 - \lambda)/p_1$ and $w_2^2 = \lambda/p_2$ where λ is swept from zero to one. Setting the weights in this way keeps the average weighting fixed at $p_1 w_1^2 + p_2 w_2^2 = 1$ and places using only samples with noise variance σ_1^2 at $\lambda = 0$ and using only samples with noise variance σ_2^2 at $\lambda = 1$. Unweighted PCA corresponds to uniform weights and occurs when $\lambda = p_2$, and inverse noise variance weights occurs when $\lambda = (p_2/\sigma_2^2)/(p_1/\sigma_1^2 + p_2/\sigma_2^2)$.

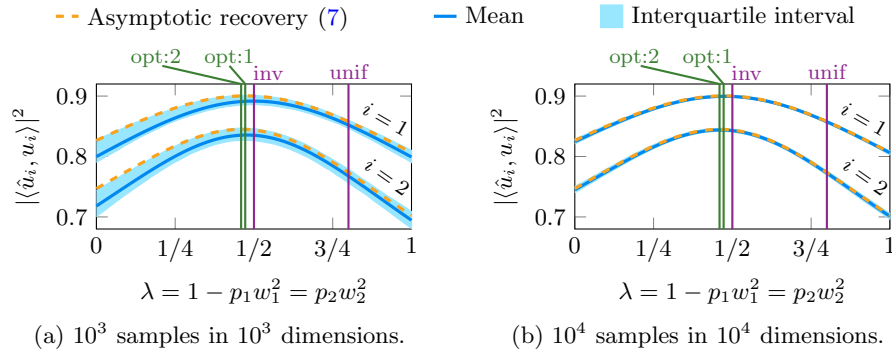


FIG 9. Simulated component recoveries $|\langle \hat{u}_i, u_i \rangle|^2$ for data generated according to the model (3) with $c = 1$ sample per dimension, underlying amplitudes $\theta_1^2 = 25$ and $\theta_2^2 = 16$, and $p_1 = 20\%$ of samples having noise variance $\sigma_1^2 = 1$ with the remaining $p_2 = 80\%$ of samples having noise variance $\sigma_2^2 = 4$. Weights are set as $w_1^2 = (1 - \lambda)/p_1$ and $w_2^2 = \lambda/p_2$. Simulation mean (blue curve) and interquartile interval (light blue ribbon) are shown with the asymptotic prediction (7) of Theorem 1 (orange dashed curve). Vertical lines indicate uniform weights (unif) for unweighted PCA, inverse noise variance weights (inv) and optimal weights (opt). Increasing the data size from (a) to (b) shrinks the interquartile intervals, indicating concentration to the mean, which is itself converging to the asymptotic recovery.

We carry out two simulations: the first has $n = 10^3$ samples in $d = 10^3$ dimensions, and the second increases these to $n = 10^4$ samples in $d = 10^4$ dimensions. Both are repeated for 500 trials. Figure 9 plots the component recoveries $|\langle \hat{u}_i, u_i \rangle|^2$ for both simulations with the mean (blue curve) and interquartile interval (light blue ribbon) shown with the asymptotic component recovery (7) of Theorem 1 (orange dashed curve). Vertical lines denote uniform weights for unweighted PCA, inverse noise variance weights and optimal weights (36). Figure 9a illustrates general agreement in behavior between the non-asymptotic recovery and its asymptotic prediction. Though the asymptotic recovery is larger than the interquartile recovery, both have the same qualitative trend. In our experience, this phenomenon occurs in general. Figure 9b shows what happens when the number of samples and dimensions are increased. The interquartile intervals shrink dramatically, indicating concentration of each component recovery (a random quantity) around its mean. Furthermore, each mean component recovery closely matches the asymptotic recovery, indicating convergence to the limit. Convergence also appears to be faster for larger λ , i.e., where more weight is given to the larger set of samples. Characterizing non-asymptotic component recoveries is an important and challenging area of future work; the agreement here gives confidence that the asymptotic predictions provide

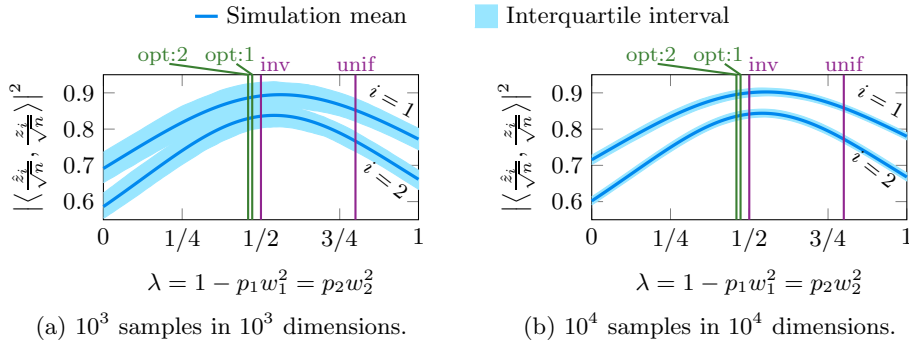


FIG 10. Simulated unweighted score recoveries $|\langle \hat{z}_i/\sqrt{n}, z_i/\sqrt{n} \rangle|^2$ for data generated according to the model (3) with $c = 1$ sample per dimension, underlying amplitudes $\theta_1^2 = 25$ and $\theta_2^2 = 16$, and $p_1 = 20\%$ of samples having noise variance $\sigma_1^2 = 1$ with the remaining $p_2 = 80\%$ of samples having noise variance $\sigma_2^2 = 4$. Weights are set as $w_1^2 = (1-\lambda)/p_1$ and $w_2^2 = \lambda/p_2$. Simulation mean (blue curve) and interquartile interval (light blue ribbon) are shown with vertical lines indicating uniform weights (unif) that correspond to unweighted PCA, inverse noise variance weights (inv), and weights that optimize component recovery (opt). The peak score recovery shown here occurs at a slightly larger λ than the peak component recovery in Fig. 9, but they have otherwise similar behavior.

meaningful insights for finite dimensions. In this setting, for example, it was significantly suboptimal to use unweighted PCA or to use only some of the samples, and using inverse noise variance weights was close to optimal. Appendix D shows analogous plots for the amplitudes $\hat{\theta}_i^2$, weighted score recoveries $|\langle \hat{z}_i/\sqrt{n}, z_i/\sqrt{n} \rangle_{\mathbf{W}^2}|^2$ and products $\langle \hat{u}_i, u_i \rangle \langle \hat{z}_i/\sqrt{n}, z_i/\sqrt{n} \rangle_{\mathbf{W}^2}^*$.

Figure 10 plots the unweighted score recoveries $|\langle \hat{z}_i/\sqrt{n}, z_i/\sqrt{n} \rangle|^2$. Though Theorem 1 does not provide their asymptotic counterparts, one might expect that they have similar behavior to the component recoveries. Better component recoveries should generally lead to better score recoveries. Comparing with Fig. 9, the peak occurs for slightly larger λ indicating better performance when slightly more weight is given to the larger set of samples, but has an otherwise similar shape and trend, as well as statistical concentration. Hence, the asymptotic component recovery (7) of Theorem 1 also provides some insight into how well the underlying scores are recovered. Note that normalizing the weights to fix the average $p_1 w_1^2 + p_2 w_2^2$ is critical for these comparisons since, e.g., doubling the weights effectively halves the resulting scores and hence halves the resulting unweighted recoveries $|\langle \hat{z}_i/\sqrt{n}, z_i/\sqrt{n} \rangle|^2$.

10. Discussion and future work. This paper analyzes weighted PCA in the high-dimensional asymptotic regime where both the number of sam-

ples n and ambient dimension d grow. We provide expressions for the asymptotic recovery of underlying amplitudes θ_i^2 , components u_i and scores z_i by the WPCA amplitudes $\hat{\theta}_i^2$, components \hat{u}_i and scores \hat{z}_i . These expressions provide new insight into how weighting affects the performance of PCA, and also led to weights that optimize the recovery of an underlying component. We also use the analysis to investigate how to optimize sampling strategies under budget constraints.

An interesting avenue of future work is further study of the benefits of optimal weighting, e.g., to characterize when optimal weights provide significant benefit over inverse noise variance or square inverse noise variance weights. A benefit of such weights over the optimal choice is that they are independent of the underlying amplitude θ_i^2 . Another interesting direction is to estimate the underlying amplitudes from the data, e.g., using (4) in Theorem 1. Likewise, estimating noise variances could aid many important applications. Incorporating spectrum estimation methods such as [16, 18] is a promising approach, and one might further exploit knowledge of which samples share a noise variance by considering the spectrums of subsets of data. Finally, alternating between estimating components using weighted PCA and estimating noise variances can help mitigate interference from large principal components. Investigating these various approaches is ongoing and future work.

Extending the analysis here to more general forms of weighted PCA is another interesting and nontrivial direction. In particular, one might consider weighting that is across variables in addition to across samples, e.g., to handle heterogeneous amounts of noise among the variables. Such analysis could also provide insight into the common preprocessing step of standardizing the variables to have unit variance. One might also consider a variant of (1) with a general weighted orthonormality in place of \mathbf{W}^2 . Developing and studying alternative ways to account for heteroscedasticity in PCA is also an interesting avenue of future work. For example, one might consider a probabilistic PCA [24] approach that accounts for heteroscedasticity; the nonuniform noise variances complicate the resulting optimization, making algorithm development for this approach nontrivial and interesting.

Finally, considering broader types of heterogeneity is an important area of future work. Increasingly, data from multiple sources are combined to find latent phenomenon so investigating how to fully utilize the available data is important both for furthering our understanding and for developing practical guidelines.

APPENDIX A: PROOF OF THEOREM 1

The model (3) for the data matrix $\mathbf{Y} := (y_1, \dots, y_n) \in \mathbb{C}^{d \times n}$ is the low-rank perturbation of a random matrix

$$(55) \quad \begin{aligned} \mathbf{Y} &= \underbrace{(u_1, \dots, u_k)}_{\mathbf{U} \in \mathbb{C}^{d \times k}} \underbrace{\text{diag}(\theta_1, \dots, \theta_k)}_{\mathbf{\Theta} \in \mathbb{R}^{k \times k}} \underbrace{(z_1, \dots, z_k)}_{\mathbf{Z} \in \mathbb{R}^{n \times k}}^{\text{H}} \\ &\quad + \underbrace{(\varepsilon_1, \dots, \varepsilon_n)}_{\mathbf{E} \in \mathbb{C}^{d \times n}} \underbrace{\text{diag}(\eta_1, \dots, \eta_n)}_{\mathbf{H} \in \mathbb{C}^{n \times n}} \\ &= \mathbf{U}\mathbf{\Theta}\mathbf{Z}^{\text{H}} + \mathbf{E}\mathbf{H}, \end{aligned}$$

The weighted PCA components $\hat{u}_1, \dots, \hat{u}_k$, amplitudes $\hat{\theta}_1, \dots, \hat{\theta}_k$, and normalized weighted scores $\mathbf{W}\hat{z}_1/\sqrt{n}, \dots, \mathbf{W}\hat{z}_k/\sqrt{n}$ are, respectively, principal left singular vectors, singular values, and right singular vectors of the normalized and weighted data matrix

$$(56) \quad \tilde{\mathbf{Y}} := \frac{1}{\sqrt{n}} \mathbf{Y} \underbrace{\text{diag}(\omega_1^2, \dots, \omega_n^2)}_{\mathbf{W} \in \mathbb{R}^{n \times n}} = \mathbf{U}\mathbf{\Theta}\tilde{\mathbf{Z}}^{\text{H}}\mathbf{W} + \tilde{\mathbf{E}},$$

where $\tilde{\mathbf{Z}} := \mathbf{Z}/\sqrt{n}$ are normalized underlying scores and $\tilde{\mathbf{E}} := \mathbf{E}\mathbf{H}\mathbf{W}/\sqrt{n}$ are normalized and weighted noise.

Without loss of generality, suppose that the components $\mathbf{U} := (u_1, \dots, u_k)$ are randomly generated according to the ‘‘orthonormalized model’’ of [4, Section 2.1]; since the noise vectors are unitarily invariant, this assumption is equivalent to considering a random rotation of data from a deterministic \mathbf{U} as done in [11, Section 5.1]. The normalized scores $\tilde{\mathbf{Z}} = (z_1/\sqrt{n}, \dots, z_k/\sqrt{n})$ are generated according to the ‘‘iid model’’ of [4, Section 2.1], and \mathbf{E} has iid entries with zero mean, unit variance and bounded fourth moment. Finally, $\mathbf{H}\mathbf{W}$ is a non-random diagonal nonnegative definite matrix with bounded spectral norm and limiting eigenvalue distribution $p_1\delta_{\omega_1^2\sigma_1^2} + \dots + p_L\delta_{\omega_L^2\sigma_L^2}$, where δ_x denotes the Dirac delta distribution at x .

A roadmap for the proof is as follows:

- (A.1) State some preliminary results on $\tilde{\mathbf{E}}$ that, taken with Lemma 5, provide a foundation for the remainder of the analysis.
- (A.2) Extend [4, Theorem 2.9] to find asymptotic weighted PCA amplitudes.
- (A.3) Extend [4, Theorem 2.10] to find asymptotic component recovery and asymptotic weighted score recovery.
- (A.4) Similar to [11, Sections 5.2–5.6], find algebraic descriptions for the expressions derived in Appendix A.2 and Appendix A.3. The original expressions are challenging to evaluate and analyze.

Unless otherwise specified, limits are as $n, d \rightarrow \infty$. Lemma 5 was crucial to carrying out the above extensions, and its proof (Appendix B) is one of our main technical contributions.

A.1. Preliminary results on $\tilde{\mathbf{E}}$. The normalized and weighted noise matrix $\tilde{\mathbf{E}}$ fits within the random matrix model studied in [3, Chapters 4, 6]. In particular, from [3, Theorem 4.3] and [3, Corollary 6.6] we conclude that the singular value distribution of $\tilde{\mathbf{E}}$ converges weakly almost surely to a nonrandom compactly supported measure $\mu_{\tilde{\mathbf{E}}}$, and the largest singular value of $\tilde{\mathbf{E}}$ converges almost surely to the supremum b of the support of $\mu_{\tilde{\mathbf{E}}}$.

It follows then that

$$(57) \quad \frac{1}{d} \operatorname{tr} \zeta (\zeta^2 \mathbf{I} - \tilde{\mathbf{E}} \tilde{\mathbf{E}}^H)^{-1} \xrightarrow{\text{a.s.}} \varphi_1(\zeta) := \int \frac{\zeta}{\zeta^2 - t^2} d\mu_{\tilde{\mathbf{E}}}(t),$$

where the convergence is uniform on $\{\zeta \in \mathbb{C} : \Re(\zeta) > b + \tau\}$ for any $\tau > 0$. Furthermore, for any $\zeta \in \mathbb{C}$ with $\Re(\zeta) > b$,

$$(58) \quad \frac{\partial}{\partial \zeta} \frac{1}{d} \operatorname{tr} \zeta (\zeta^2 \mathbf{I} - \tilde{\mathbf{E}} \tilde{\mathbf{E}}^H)^{-1} \xrightarrow{\text{a.s.}} \varphi_1'(\zeta).$$

We conclude the preliminaries by verifying some properties of φ_1 .

- a) For any $\zeta > b$, the integrand in (57) is positive and bounded away from zero since the support of $\mu_{\tilde{\mathbf{E}}}$ lies between zero and b .
Thus, $\forall \zeta > b$ $\varphi_1(\zeta) > 0$.
- b) As $|\zeta| \rightarrow \infty$, the integrand in (57) goes to zero uniformly in t .
Thus, $\varphi_1(\zeta) \rightarrow 0$ as $|\zeta| \rightarrow \infty$.
- c) The imaginary part of $\varphi_1(\zeta)$ is

$$\Im\{\varphi_1(\zeta)\} = \int \Im\left(\frac{\zeta}{\zeta^2 - t^2}\right) d\mu_{\tilde{\mathbf{E}}}(t) = -\Im(\zeta) \underbrace{\int \frac{|\zeta|^2 + t^2}{|\zeta^2 - t^2|^2} d\mu_{\tilde{\mathbf{E}}}(t)}_{>0}.$$

Thus, $\varphi_1(\zeta) \in \mathbb{R} \Leftrightarrow \zeta \in \mathbb{R}$.

Lemma 5 establishes the analogous results for the weighted trace.

A.2. Largest singular values. This section extends [4, Theorem 2.9] to find the limiting largest singular values of the weighted matrix $\tilde{\mathbf{Y}}$ in (56). As in [4, Section 4], $\liminf \hat{\theta}_i \geq b$ almost surely for each $i \in \{1, \dots, k\}$ so we focus on singular values larger than $b + \tau$ where $\tau > 0$ is arbitrary. The following lemma generalizes [4, Lemma 4.1] to account for the weights.

LEMMA 9. *Let $\zeta > 0$ be arbitrary but not a singular value of $\tilde{\mathbf{E}}$. Then ζ is a singular value of $\tilde{\mathbf{Y}} = \mathbf{U}\Theta\tilde{\mathbf{Z}}^H\mathbf{W} + \tilde{\mathbf{E}}$ if and only if the following matrix is singular:*

$$(59) \quad \mathbf{M}(\zeta) := \begin{bmatrix} \mathbf{U}^H\zeta(\zeta^2\mathbf{I} - \tilde{\mathbf{E}}\tilde{\mathbf{E}}^H)^{-1}\mathbf{U} & \mathbf{U}^H(\zeta^2\mathbf{I} - \tilde{\mathbf{E}}\tilde{\mathbf{E}}^H)^{-1}\tilde{\mathbf{E}}\mathbf{W}\tilde{\mathbf{Z}} \\ \tilde{\mathbf{Z}}^H\mathbf{W}\tilde{\mathbf{E}}^H(\zeta^2\mathbf{I} - \tilde{\mathbf{E}}\tilde{\mathbf{E}}^H)^{-1}\mathbf{U} & \tilde{\mathbf{Z}}^H\zeta\mathbf{W}(\zeta^2\mathbf{I} - \tilde{\mathbf{E}}\tilde{\mathbf{E}}^H)^{-1}\mathbf{W}\tilde{\mathbf{Z}} \\ - \begin{bmatrix} \Theta^{-1} & \Theta^{-1} \end{bmatrix} \end{bmatrix}.$$

Lemma 9 is proved in the same way as [4, Lemma 4.1] but with the weights incorporated; for convenience, we state it here with some additional detail.

PROOF OF LEMMA 9. By [12, Theorem 7.3.3], ζ is a singular value of $\tilde{\mathbf{Y}}$ if and only if it is a root of the characteristic polynomial

$$(60) \quad 0 = \det \left\{ \zeta\mathbf{I} - \begin{pmatrix} & \tilde{\mathbf{Y}} \\ \tilde{\mathbf{Y}}^H & \end{pmatrix} \right\}$$

$$(61) \quad = \det \left\{ \zeta\mathbf{I} - \begin{pmatrix} & \tilde{\mathbf{E}} \\ \tilde{\mathbf{E}}^H & \end{pmatrix} - \begin{pmatrix} \mathbf{U} & \\ & \mathbf{W}\tilde{\mathbf{Z}} \end{pmatrix} \begin{pmatrix} \Theta & \Theta \\ & \Theta \end{pmatrix} \begin{pmatrix} \mathbf{U} & \\ & \mathbf{W}\tilde{\mathbf{Z}} \end{pmatrix}^H \right\}$$

$$(62) \quad = \det \left\{ \zeta\mathbf{I} - \begin{pmatrix} & \tilde{\mathbf{E}} \\ \tilde{\mathbf{E}}^H & \end{pmatrix} \right\} \det \begin{pmatrix} \Theta & \Theta \\ \Theta & \Theta \end{pmatrix} \det\{-\mathbf{M}(\zeta)\},$$

where (61) is a convenient form of the matrix, and (62) follows from the determinant identity

$$(63) \quad \det(\mathbf{A} - \mathbf{BDC}) = \det(\mathbf{A}) \det(\mathbf{D}) \det(\mathbf{D}^{-1} - \mathbf{CA}^{-1}\mathbf{B}),$$

for invertible matrices \mathbf{A} and \mathbf{D} and the block matrix inverse [12, Equation (0.7.3.1)]

$$(64) \quad \left\{ \zeta\mathbf{I} - \begin{pmatrix} & \tilde{\mathbf{E}} \\ \tilde{\mathbf{E}}^H & \end{pmatrix} \right\}^{-1} = \begin{Bmatrix} \zeta(\zeta^2\mathbf{I} - \tilde{\mathbf{E}}\tilde{\mathbf{E}}^H)^{-1} & (\zeta^2\mathbf{I} - \tilde{\mathbf{E}}\tilde{\mathbf{E}}^H)^{-1}\tilde{\mathbf{E}} \\ \tilde{\mathbf{E}}^H(\zeta^2\mathbf{I} - \tilde{\mathbf{E}}\tilde{\mathbf{E}}^H)^{-1} & \zeta(\zeta^2\mathbf{I} - \tilde{\mathbf{E}}\tilde{\mathbf{E}}^H)^{-1} \end{Bmatrix}.$$

Note that (64) is invertible because ζ is not a singular value of $\tilde{\mathbf{E}}$. As a further consequence, (62) is zero exactly when $\mathbf{M}(\zeta)$ is singular. \square

Applying Ascoli's theorem, [4, Proposition A.2], (57) and Lemma 5 yields

$$(65) \quad \mathbf{M}(\zeta) \xrightarrow{\text{a.s.}} \tilde{\mathbf{M}}(\zeta) := \begin{pmatrix} \varphi_1(\zeta)\mathbf{I}_k & \\ & \varphi_2(\zeta)\mathbf{I}_k \end{pmatrix} - \begin{pmatrix} \Theta^{-1} & \Theta^{-1} \\ \Theta^{-1} & \Theta^{-1} \end{pmatrix},$$

where the convergence is uniform on $\{\zeta \in \mathbb{C} : \Re(\zeta) > b + \tau\}$. Finally, applying [4, Lemma A.1] in the same way as [4, Section 4] yields

$$(66) \quad \hat{\theta}_i^2 \xrightarrow{\text{a.s.}} \begin{cases} \rho_i^2 & \text{if } \theta_i^2 > \bar{\theta}^2, \\ b^2 & \text{otherwise,} \end{cases} =: r_i^{(\theta)}$$

where $D(\zeta) := \varphi_1(\zeta)\varphi_2(\zeta)$ for $\zeta > b$, $\rho_i := D^{-1}(1/\theta_i^2)$, $\bar{\theta}^2 := 1/D(b^+)$, and $f(b^+) := \lim_{\zeta \rightarrow b^+} f(\zeta)$ denotes a limit from above.

A.3. Recovery of singular vectors. This section extends [4, Theorem 2.10] to find the limiting recovery of singular vectors. Suppose $\theta_i > \bar{\theta}$. Then $\hat{\theta}_i \xrightarrow{\text{a.s.}} \rho_i > b$ and so, almost surely, $\hat{\theta}_i > \|\tilde{\mathbf{E}}\|$ eventually. Namely, $\hat{\theta}_i$ is almost surely eventually not a singular value of $\tilde{\mathbf{E}}$. The following lemma generalizes [4, Lemma 5.1] to account for the weights.

LEMMA 10. *Suppose $\hat{\theta}_i$ is not a singular value of $\tilde{\mathbf{E}}$. Then*

$$(67) \quad \mathbf{M}(\hat{\theta}_i) \begin{pmatrix} \Theta \tilde{\mathbf{Z}}^H \mathbf{W}^2 \hat{z}_i / \sqrt{n} \\ \Theta \mathbf{U}^H \hat{u}_i \end{pmatrix} = 0,$$

and

$$(68) \quad 1 = \chi_1 + \chi_2 + 2\Re(\chi_3),$$

where $\mathbf{\Gamma} := (\hat{\theta}_i^2 \mathbf{I} - \tilde{\mathbf{E}}\tilde{\mathbf{E}}^H)^{-1}$ and

$$(69) \quad \begin{aligned} \chi_1 &:= \sum_{j_1, j_2=1}^k \theta_{j_1} \theta_{j_2} \left\langle \frac{\hat{z}_i}{\sqrt{n}}, \frac{z_{j_1}}{\sqrt{n}} \right\rangle_{\mathbf{W}^2} \left\langle \frac{\hat{z}_i}{\sqrt{n}}, \frac{z_{j_2}}{\sqrt{n}} \right\rangle_{\mathbf{W}^2}^* u_{j_2}^H \hat{\theta}_i^2 \mathbf{\Gamma}^2 u_{j_1}, \\ \chi_2 &:= \sum_{j_1, j_2=1}^k \theta_{j_1} \theta_{j_2} \langle \hat{u}_i, u_{j_1} \rangle \langle \hat{u}_i, u_{j_2} \rangle^* \hat{z}_{j_2}^H \mathbf{W} \tilde{\mathbf{E}}^H \mathbf{\Gamma}^2 \tilde{\mathbf{E}} \mathbf{W} \hat{z}_{j_1}, \\ \chi_3 &:= \sum_{j_1, j_2=1}^k \theta_{j_1} \theta_{j_2} \langle \hat{u}_i, u_{j_1} \rangle \left\langle \frac{\hat{z}_i}{\sqrt{n}}, \frac{z_{j_2}}{\sqrt{n}} \right\rangle_{\mathbf{W}^2}^* u_{j_2}^H \hat{\theta}_i \mathbf{\Gamma}^2 \tilde{\mathbf{E}} \mathbf{W} \hat{z}_{j_1}. \end{aligned}$$

Lemma 10 is proved in the same way as [4, Lemma 5.1] but with the weights incorporated.

PROOF OF LEMMA 10. Let $\tilde{\mathbf{X}} := \mathbf{U}\Theta\tilde{\mathbf{Z}}^H\mathbf{W}$ be the weighted and normal-

ized underlying data. Substituting (59) into (67) and factoring yields

$$(70) \quad \mathbf{M}(\hat{\theta}_i) \begin{bmatrix} \Theta \tilde{\mathbf{Z}}^H \mathbf{W}^2 \hat{z}_i / \sqrt{n} \\ \Theta \mathbf{U}^H \hat{u}_i \end{bmatrix}$$

$$(71) \quad = \begin{bmatrix} \mathbf{U}^H \{ (\hat{\theta}_i^2 \mathbf{I} - \tilde{\mathbf{E}} \tilde{\mathbf{E}}^H)^{-1} (\hat{\theta}_i \tilde{\mathbf{X}} \mathbf{W} \hat{z}_i / \sqrt{n} + \tilde{\mathbf{E}} \tilde{\mathbf{X}}^H \hat{u}_i) - \hat{u}_i \} \\ \tilde{\mathbf{Z}}^H \mathbf{W} \{ (\hat{\theta}_i^2 \mathbf{I} - \tilde{\mathbf{E}}^H \tilde{\mathbf{E}})^{-1} (\tilde{\mathbf{E}}^H \tilde{\mathbf{X}} \mathbf{W} \hat{z}_i / \sqrt{n} + \hat{\theta}_i \tilde{\mathbf{X}}^H \hat{u}_i) - \mathbf{W} \hat{z}_i / \sqrt{n} \} \end{bmatrix}$$

$$(72) \quad = \begin{bmatrix} \mathbf{U}^H (\hat{u}_i - \hat{u}_i) \\ \tilde{\mathbf{Z}}^H \mathbf{W} (\mathbf{W} \hat{z}_i / \sqrt{n} - \mathbf{W} \hat{z}_i / \sqrt{n}) \end{bmatrix} = 0$$

where (71) uses the matrix identity $\tilde{\mathbf{E}}^H (\hat{\theta}_i^2 \mathbf{I} - \tilde{\mathbf{E}} \tilde{\mathbf{E}}^H)^{-1} = (\hat{\theta}_i^2 \mathbf{I} - \tilde{\mathbf{E}}^H \tilde{\mathbf{E}})^{-1} \tilde{\mathbf{E}}^H$, and (72) follows by substituting $\tilde{\mathbf{X}} = \tilde{\mathbf{Y}} - \tilde{\mathbf{E}}$ and using the singular vector identities

$$(73) \quad \tilde{\mathbf{Y}} \mathbf{W} \hat{z}_i / \sqrt{n} = \hat{\theta}_i \hat{u}_i, \quad \tilde{\mathbf{Y}}^H \hat{u}_i = \hat{\theta}_i \mathbf{W} \hat{z}_i / \sqrt{n}.$$

To obtain (68), reuse the identity $\hat{u}_i = (\hat{\theta}_i^2 \mathbf{I} - \tilde{\mathbf{E}} \tilde{\mathbf{E}}^H)^{-1} (\hat{\theta}_i \tilde{\mathbf{X}} \mathbf{W} \hat{z}_i / \sqrt{n} + \tilde{\mathbf{E}} \tilde{\mathbf{X}}^H \hat{u}_i)$ used to obtain (72) and expand as

$$(74) \quad 1 = \hat{u}_i^H \hat{u}_i \\ = \left(\hat{\theta}_i \tilde{\mathbf{X}} \mathbf{W} \frac{\hat{z}_i}{\sqrt{n}} + \tilde{\mathbf{E}} \tilde{\mathbf{X}}^H \hat{u}_i \right)^H (\hat{\theta}_i^2 \mathbf{I} - \tilde{\mathbf{E}} \tilde{\mathbf{E}}^H)^{-2} \left(\hat{\theta}_i \tilde{\mathbf{X}} \mathbf{W} \frac{\hat{z}_i}{\sqrt{n}} + \tilde{\mathbf{E}} \tilde{\mathbf{X}}^H \hat{u}_i \right) \\ = \chi_1 + \chi_2 + 2\Re(\chi_3),$$

where the outer terms are

$$(75) \quad \chi_1 := \frac{\hat{z}_i^H}{\sqrt{n}} \mathbf{W} \tilde{\mathbf{X}}^H \hat{\theta}_i^2 \Gamma^2 \tilde{\mathbf{X}} \mathbf{W} \frac{\hat{z}_i}{\sqrt{n}}, \quad \chi_2 := \hat{u}_i^H \tilde{\mathbf{X}} \tilde{\mathbf{E}}^H \Gamma^2 \tilde{\mathbf{E}} \tilde{\mathbf{X}}^H \hat{u}_i,$$

and the cross term is

$$(76) \quad \chi_3 := \frac{\hat{z}_i^H}{\sqrt{n}} \mathbf{W} \tilde{\mathbf{X}}^H \hat{\theta}_i \Gamma^2 \tilde{\mathbf{E}} \tilde{\mathbf{X}}^H \hat{u}_i.$$

Expanding $\tilde{\mathbf{X}} = \mathbf{U} \Theta \tilde{\mathbf{Z}}^H \mathbf{W} = \theta_1 u_1 (z_1 / \sqrt{n})^H \mathbf{W} + \cdots + \theta_k u_k (z_k / \sqrt{n})^H \mathbf{W}$ in the terms (75)–(76) and simplifying yields (69). \square

Applying the convergence $\mathbf{M}(\hat{\theta}_i) \xrightarrow{\text{a.s.}} \tilde{\mathbf{M}}(\rho_i)$ to (67) in Lemma 10 yields

$$(77) \quad \begin{pmatrix} \xi \\ \delta \end{pmatrix} := \text{proj}_{\{\ker \tilde{\mathbf{M}}(\rho_i)\}^\perp} \begin{pmatrix} \Theta \tilde{\mathbf{Z}}^H \mathbf{W}^2 \hat{z}_i / \sqrt{n} \\ \Theta \mathbf{U}^H \hat{u}_i \end{pmatrix} \xrightarrow{\text{a.s.}} 0.$$

Observe next that, similar to [4, Section 5],

$$(78) \quad \ker \tilde{\mathbf{M}}(\rho_i) = \left\{ \begin{pmatrix} s \\ t \end{pmatrix} \in \mathbb{C}^{2k} : \begin{array}{ll} t_j = s_j = 0 & \text{if } \theta_j \neq \theta_i \\ t_j = \theta_i \varphi_1(\rho_i) s_j & \text{if } \theta_j = \theta_i \end{array} \right\},$$

so the projection entries are

$$(79) \quad \begin{pmatrix} \xi_j \\ \delta_j \end{pmatrix} = \theta_j \begin{pmatrix} \langle \hat{z}_i / \sqrt{n}, z_j / \sqrt{n} \rangle_{\mathbf{W}^2} \\ \langle \hat{u}_i, u_j \rangle \end{pmatrix},$$

for j such that $\theta_j \neq \theta_i$, and

$$(80) \quad \begin{pmatrix} \xi_j \\ \delta_j \end{pmatrix} = \left\{ \theta_i \varphi_1(\rho_i) \left\langle \frac{\hat{z}_i}{\sqrt{n}}, \frac{z_j}{\sqrt{n}} \right\rangle_{\mathbf{W}^2} - \langle \hat{u}_i, u_j \rangle \right\} \frac{\theta_i}{\theta_i^2 \varphi_1^2(\rho_i) + 1} \begin{pmatrix} \theta_i \varphi_1(\rho_i) \\ -1 \end{pmatrix},$$

for j such that $\theta_j = \theta_i$. Applying the convergence (77) to (79) yields

$$(81) \quad \sum_{j: \theta_j \neq \theta_i} |\langle \hat{u}_i, u_j \rangle|^2 + \left| \left\langle \frac{\hat{z}_i}{\sqrt{n}}, \frac{z_j}{\sqrt{n}} \right\rangle_{\mathbf{W}^2} \right|^2 \xrightarrow{\text{a.s.}} 0,$$

and applying the convergence (77) to (80) yields

$$(82) \quad \sum_{j: \theta_j = \theta_i} \left| \sqrt{\frac{\varphi_1(\rho_i)}{\varphi_2(\rho_i)}} \left\langle \frac{\hat{z}_i}{\sqrt{n}}, \frac{z_j}{\sqrt{n}} \right\rangle_{\mathbf{W}^2} - \langle \hat{u}_i, u_j \rangle \right|^2 \xrightarrow{\text{a.s.}} 0,$$

recalling that $D(\rho_i) = \varphi_1(\rho_i)\varphi_2(\rho_i) = 1/\theta_i^2$.

Turning now to (68) in Lemma 10, note that applying [4, Proposition A.2] yields the convergence $\chi_3 \xrightarrow{\text{a.s.}} 0$ as well as the almost sure convergence to zero of the summands in (69) for χ_1 and χ_2 for which $j_1 \neq j_2$. By (81), the summands for which $\theta_{j_1}, \theta_{j_2} \neq \theta_i$ also converge almost surely to zero.

Furthermore, by (58) and Lemma 5

$$\begin{aligned}
(83) \quad \frac{1}{d} \operatorname{tr} \hat{\theta}_i^2 \Gamma^2 &= \frac{1}{d} \operatorname{tr} \zeta^2 (\zeta^2 \mathbf{I} - \tilde{\mathbf{E}} \tilde{\mathbf{E}}^H)^{-2} \Big|_{\zeta=\hat{\theta}_i} \\
&= \left(\frac{1}{2\zeta} - \frac{1}{2} \frac{\partial}{\partial \zeta} \right) \left\{ \frac{1}{d} \operatorname{tr} \zeta (\zeta^2 \mathbf{I} - \tilde{\mathbf{E}} \tilde{\mathbf{E}}^H)^{-1} \right\} \Big|_{\zeta=\hat{\theta}_i} \\
&\xrightarrow{\text{a.s.}} \frac{\varphi_1(\rho_i)}{2\rho_i} - \frac{\varphi_1'(\rho_i)}{2}, \\
(84) \quad \frac{1}{n} \operatorname{tr} \mathbf{W} \tilde{\mathbf{E}}^H \Gamma^2 \tilde{\mathbf{E}} \mathbf{W} &= \frac{1}{n} \operatorname{tr} \mathbf{W} \tilde{\mathbf{E}}^H (\zeta^2 \mathbf{I} - \tilde{\mathbf{E}} \tilde{\mathbf{E}}^H)^{-2} \tilde{\mathbf{E}} \mathbf{W} \Big|_{\zeta=\hat{\theta}_i} \\
&= \left(-\frac{1}{2\zeta} - \frac{1}{2} \frac{\partial}{\partial \zeta} \right) \left\{ \frac{1}{n} \operatorname{tr} \zeta \mathbf{W} (\zeta^2 \mathbf{I} - \tilde{\mathbf{E}} \tilde{\mathbf{E}}^H)^{-1} \mathbf{W} \right\} \Big|_{\zeta=\hat{\theta}_i} \\
&\xrightarrow{\text{a.s.}} -\frac{\varphi_2(\rho_i)}{2\rho_i} - \frac{\varphi_2'(\rho_i)}{2},
\end{aligned}$$

so applying [4, Proposition A.2] once more we have

$$\begin{aligned}
(85) \quad \chi_1 &= \theta_i^2 \left\{ \frac{\varphi_1(\rho_i)}{2\rho_i} - \frac{\varphi_1'(\rho_i)}{2} \right\} \sum_{j:\theta_j=\theta_i} \left| \left\langle \frac{\hat{z}_i}{\sqrt{n}}, \frac{z_j}{\sqrt{n}} \right\rangle_{\mathbf{W}^2} \right|^2 + o(1), \\
\chi_2 &= \theta_i^2 \left\{ -\frac{\varphi_2(\rho_i)}{2\rho_i} - \frac{\varphi_2'(\rho_i)}{2} \right\} \sum_{j:\theta_j=\theta_i} |\langle \hat{u}_i, u_j \rangle|^2 + o(1),
\end{aligned}$$

where $o(1)$ denotes a sequence that almost surely converges to zero. Combining (68), (82) and (85) yields

$$\begin{aligned}
(86) \quad 1 &= -\frac{\theta_i^2 D'(\rho_i)}{2\varphi_1(\rho_i)} \sum_{j:\theta_j=\theta_i} |\langle \hat{u}_i, u_j \rangle|^2 + o(1), \\
1 &= -\frac{\theta_i^2 D'(\rho_i)}{2\varphi_2(\rho_i)} \sum_{j:\theta_j=\theta_i} \left| \left\langle \frac{\hat{z}_i}{\sqrt{n}}, \frac{z_j}{\sqrt{n}} \right\rangle_{\mathbf{W}^2} \right|^2 + o(1),
\end{aligned}$$

where we use the fact that $D'(\zeta) = \varphi_1'(\zeta)\varphi_2(\zeta) + \varphi_1(\zeta)\varphi_2'(\zeta)$. Solving (86)

for the recoveries and recalling (81) yields

$$(87) \quad \sum_{j:\theta_j=\theta_i} |\langle \hat{u}_i, u_j \rangle|^2 \xrightarrow{\text{a.s.}} \frac{-2\varphi_1(\rho_i)}{\theta_i^2 D'(\rho_i)} =: r_i^{(u)},$$

$$(88) \quad \sum_{j:\theta_j=\theta_i} \left| \left\langle \frac{\hat{z}_i}{\sqrt{n}}, \frac{z_j}{\sqrt{n}} \right\rangle_{\mathbf{W}^2} \right|^2 \xrightarrow{\text{a.s.}} \frac{-2\varphi_2(\rho_i)}{\theta_i^2 D'(\rho_i)} =: r_i^{(z)},$$

$$(89) \quad \sum_{j:\theta_j \neq \theta_i} |\langle \hat{u}_i, u_j \rangle|^2, \quad \sum_{j:\theta_j \neq \theta_i} \left| \left\langle \frac{\hat{z}_i}{\sqrt{n}}, \frac{z_j}{\sqrt{n}} \right\rangle_{\mathbf{W}^2} \right|^2 \xrightarrow{\text{a.s.}} 0.$$

Furthermore, combining (82) and (86) yields

$$(90) \quad \sum_{j:\theta_j=\theta_i} \langle \hat{u}_i, u_j \rangle \left\langle \frac{\hat{z}_i}{\sqrt{n}}, \frac{z_j}{\sqrt{n}} \right\rangle_{\mathbf{W}^2}^* \xrightarrow{\text{a.s.}} \frac{-2\varphi_1(\rho_i)}{\theta_i^2 D'(\rho_i)} \sqrt{\frac{\varphi_2(\rho_i)}{\varphi_1(\rho_i)}} = \sqrt{r_i^{(u)} r_i^{(z)}}.$$

A.4. Algebraic description. This section concludes the proof by finding algebraic descriptions of the almost sure limits (66), (87)–(88) and (90). As in [11, Section 5.2], we change variables to

$$(91) \quad \psi(\zeta) := \frac{c\zeta}{\varphi_1(\zeta)} = \left\{ \frac{1}{c} \int \frac{d\mu_{\hat{\mathbf{E}}}(t)}{\zeta^2 - t^2} \right\}^{-1},$$

and observe that analogously to [11, Section 5.3] ψ has the properties:

a) $0 = Q(\psi(\zeta), \zeta)$ for all $\zeta > b$ where

$$(92) \quad Q(s, \zeta) := \frac{c\zeta^2}{s^2} + \frac{c-1}{s} - c \sum_{\ell=1}^L \frac{p_\ell}{s - w_\ell^2 \sigma_\ell^2},$$

and the inverse function is given by

$$(93) \quad \psi^{-1}(x) = \sqrt{\frac{x}{c} \left(1 + c \sum_{\ell=1}^L \frac{p_\ell w_\ell^2 \sigma_\ell^2}{x - w_\ell^2 \sigma_\ell^2} \right)} = \sqrt{\frac{x C(x)}{c}},$$

where C is defined in (6);

b) $\max_\ell (w_\ell^2 \sigma_\ell^2) < \psi(\zeta) < c\zeta^2$;

c) $0 < \psi(b^+) < \infty$ and $\psi'(b^+) = \infty$.

Expressing D in terms of ψ yields

$$(94) \quad D(\zeta) = \varphi_1(\zeta) \sum_{\ell=1}^L \frac{p_\ell w_\ell^2}{\zeta - w_\ell^2 \sigma_\ell^2 \varphi_1(\zeta)/c} = c \sum_{\ell=1}^L \frac{p_\ell w_\ell^2}{\psi(\zeta) - w_\ell^2 \sigma_\ell^2} = \frac{1 - B_i(\psi(\zeta))}{\theta_i^2},$$

and

$$(95) \quad \frac{D'(\zeta)}{\zeta} = -\frac{c\psi'(\zeta)}{\zeta} \sum_{\ell=1}^L \frac{p_\ell w_\ell^2}{\{\psi(\zeta) - w_\ell^2 \sigma_\ell^2\}^2} = -\frac{2c}{\theta_i^2} \frac{B_i'(\psi(\zeta))}{A(\psi(\zeta))},$$

where A and B_i are defined in (5) and the second equality in (95) follows analogously to [11, Section 5.4] by deriving the identity

$$(96) \quad \psi'(\zeta) = \frac{2c\zeta}{A(\psi(\zeta))},$$

from Property (a) then simplifying.

Rearranging (96) then applying Property (c) yields

$$(97) \quad A(\psi(b^+)) = \frac{2cb}{\psi'(b^+)} = 0,$$

so $\psi(b^+)$ is a root of A . If $\theta_i^2 > \bar{\theta}^2$, then $\rho_i = D^{-1}(1/\theta_i^2)$ and rearranging (94) yields

$$(98) \quad B_i(\psi(\rho_i)) = 1 - \theta_i^2 D(\rho_i) = 0,$$

so $\psi(\rho_i)$ is a root of B_i . Recall that $\psi(b^+), \psi(\rho_i) \geq \max_\ell(w_\ell^2 \sigma_\ell^2)$ by Property (b), and observe that both $A(x)$ and $B_i(x)$ monotonically increase for $x > \max_\ell(w_\ell^2 \sigma_\ell^2)$ from negative infinity to one. Thus, each has exactly one real root larger than $\max_\ell(w_\ell^2 \sigma_\ell^2)$, i.e., its largest real root, and so $\psi(b^+) = \alpha$ and $\psi(\rho_i) = \beta_i$ when $\theta_i^2 > \bar{\theta}^2$, where α and β_i are the largest real roots of A and B_i , respectively.

Even though $\psi(\rho_i)$ is defined only when $\theta_i^2 > \bar{\theta}^2$, the largest real roots α and β are always defined and always larger than $\max_\ell(w_\ell^2 \sigma_\ell^2)$. Thus

$$(99) \quad \theta_i^2 > \bar{\theta}^2 = \frac{1}{D(b^+)} = \frac{\theta_i^2}{1 - B_i(\psi(b^+))} \Leftrightarrow B_i(\alpha) < 0 \\ \Leftrightarrow \alpha < \beta_i \Leftrightarrow A(\beta_i) > 0$$

where the final equivalence holds because $A(x)$ and $B_i(x)$ are both strictly increasing functions for $x > \max_\ell(w_\ell^2 \sigma_\ell^2)$ and $A(\alpha) = B_i(\beta_i) = 0$.

Using the inverse function (93) in Property (a) and (99), write (66) as

$$(100) \quad r_i^{(\theta)} = \begin{cases} \{\psi^{-1}(\psi(\rho_i))\}^2 & \text{if } \theta_i^2 > \bar{\theta}^2, \\ \{\psi^{-1}(\psi(b))\}^2 & \text{otherwise,} \end{cases} = \begin{cases} \beta_i C(\beta_i)/c & \text{if } \alpha < \beta_i, \\ \alpha C(\alpha)/c & \text{otherwise.} \end{cases}$$

Using \max to be succinct yields (4). Likewise, rewrite (87) and (88) using ψ and (95), obtaining

$$(101) \quad r_i^{(u)} = \frac{-2\varphi_1(\rho_i)}{\theta_i^2 D'(\rho_i)} = \frac{1}{\psi(\rho_i)} \frac{A(\psi(\rho_i))}{B_i'(\psi(\rho_i))} = \frac{1}{\beta_i} \frac{A(\beta_i)}{B_i'(\beta_i)},$$

$$(102) \quad r_i^{(z)} = \frac{-2\varphi_2(\rho_i)}{\theta_i^2 D'(\rho_i)} = \frac{\varphi_2(\rho_i)}{c\rho_i} \frac{A(\psi(\rho_i))}{B_i'(\psi(\rho_i))} = \frac{\varphi_1(\rho_i)\varphi_2(\rho_i)}{c\rho_i\varphi_1(\rho_i)} \frac{A(\psi(\rho_i))}{B_i'(\psi(\rho_i))} \\ = \frac{\psi(\rho_i)}{c^2\theta_i^2\rho_i^2} \frac{A(\psi(\rho_i))}{B_i'(\psi(\rho_i))} = \frac{1}{c\theta_i^2 C(\beta_i)} \frac{A(\psi(\rho_i))}{B_i'(\psi(\rho_i))},$$

and combine with (89) to obtain (7)–(8). Taking the geometric mean likewise yields (9) as an algebraic description of the almost sure limit (90). \square

APPENDIX B: PROOF OF LEMMA 5

Unless otherwise specified, limits are as $n, d \rightarrow \infty$. Consider the expansion

$$(103) \quad \frac{1}{n} \operatorname{tr} \zeta \mathbf{W} (\zeta^2 \mathbf{I} - \tilde{\mathbf{E}}^H \tilde{\mathbf{E}})^{-1} \mathbf{W} = \sum_{\ell=1}^L \frac{n_\ell}{n} w_\ell^2 \left\{ \frac{1}{n_\ell} \operatorname{tr} \Delta_\ell(\zeta) \right\}$$

where $\Delta_\ell(\zeta) \in \mathbb{C}^{n_\ell \times n_\ell}$ is the ℓ th diagonal block of $\zeta(\zeta^2 \mathbf{I} - \tilde{\mathbf{E}}^H \tilde{\mathbf{E}})^{-1}$. The proof proceeds as follows:

(B.1) Prove that for any fixed $\zeta = r + is \in \mathbb{C}$ with $r, s \neq 0$,

$$(104) \quad \frac{1}{n_\ell} \operatorname{tr} \Delta_\ell(\zeta) \xrightarrow{\text{a.s.}} \mathbb{E} \frac{1}{n_\ell} \operatorname{tr} \Delta_\ell(\zeta).$$

(B.2) Prove that for any fixed $\zeta = r + is \in \mathbb{C}$ with $r, s \neq 0$,

$$(105) \quad \mathbb{E} \frac{1}{n_\ell} \operatorname{tr} \Delta_\ell(\zeta) \rightarrow \frac{1}{\zeta - w_\ell^2 \sigma_\ell^2 \varphi_1(\zeta)/c}.$$

(B.3) Combine (104) and (105) to obtain pointwise almost sure convergence then extend to the almost sure uniform convergence (25) and the convergence of the derivative (27) in Lemma 5.

(B.4) Prove that φ_2 has the properties (26) in Lemma 5.

(B.1)–(B.3) follows the approach of the analogous proofs in [3, Section 2.3.2]. In (B.1) and (B.2), we let $\ell = 1$ to simplify notation; the results hold for all ℓ in the same way.

B.1. Pointwise almost sure convergence to the mean. Let $\zeta = r + \iota s \in \mathbb{C}$ with $r, s \neq 0$, and consider the expansion [3, Section 2.3.2]

$$(106) \quad \frac{1}{n_1} \operatorname{tr} \mathbf{\Delta}_1(\zeta) - \mathbb{E} \frac{1}{n_1} \operatorname{tr} \mathbf{\Delta}_1(\zeta) = \sum_{i=1}^n \underbrace{(\mathbb{E}_{i-1} - \mathbb{E}_i)}_{=:\gamma_i} \left\{ \frac{1}{n_1} \operatorname{tr} \mathbf{\Delta}_1(\zeta) \right\},$$

where \mathbb{E}_i denotes expectation over the first i columns of $\tilde{\mathbf{E}}$. Note that

$$(107) \quad \begin{aligned} \operatorname{tr} \mathbf{\Delta}_1(\zeta) &= \zeta \operatorname{tr} \mathbf{\Omega} (\zeta^2 \mathbf{I} - \tilde{\mathbf{E}}^H \tilde{\mathbf{E}})^{-1} \mathbf{\Omega}^H \\ &= \zeta \left[\delta_i \{(\zeta^2 \mathbf{I} - \tilde{\mathbf{E}}^H \tilde{\mathbf{E}})^{-1}\}_{ii} + \operatorname{tr} \mathbf{\Omega}_{-i} \{(\zeta^2 \mathbf{I} - \tilde{\mathbf{E}}^H \tilde{\mathbf{E}})^{-1}\}_{-ii} \mathbf{\Omega}_{-i}^H \right] \end{aligned}$$

for each $i \in \{1, \dots, n\}$ where

- $\mathbf{\Omega} := [\mathbf{I}_{n_1 \times n_1} \mathbf{0}_{n_1 \times (n-n_1)}] \in \{0, 1\}^{n_1 \times n}$ is used to extract the first $n_1 \times n_1$ diagonal block of $(\zeta^2 \mathbf{I} - \tilde{\mathbf{E}}^H \tilde{\mathbf{E}})^{-1}$,
- δ_i is one when $i \in [1, n_1]$ and zero otherwise,
- $\{(\zeta^2 \mathbf{I} - \tilde{\mathbf{E}}^H \tilde{\mathbf{E}})^{-1}\}_{ii}$ is the i th diagonal entry of $(\zeta^2 \mathbf{I} - \tilde{\mathbf{E}}^H \tilde{\mathbf{E}})^{-1}$,
- $\mathbf{\Omega}_{-i} \in \{0, 1\}^{n_1 \times (n-1)}$ is $\mathbf{\Omega}$ with the i th column removed, and
- $\{(\zeta^2 \mathbf{I} - \tilde{\mathbf{E}}^H \tilde{\mathbf{E}})^{-1}\}_{-ii}$ is $(\zeta^2 \mathbf{I} - \tilde{\mathbf{E}}^H \tilde{\mathbf{E}})^{-1}$ with both the i th column and the i th row removed.

Taking block matrix inverses [12, Equation (0.7.3.1)] yields

$$(108) \quad \{(\zeta^2 \mathbf{I} - \tilde{\mathbf{E}}^H \tilde{\mathbf{E}})^{-1}\}_{ii} = \frac{1}{\zeta^2 - \tilde{\varepsilon}_i^H \tilde{\varepsilon}_i - \tilde{\varepsilon}_i^H \tilde{\mathbf{E}}_{-i} (\zeta^2 \mathbf{I} - \tilde{\mathbf{E}}_{-i}^H \tilde{\mathbf{E}}_{-i})^{-1} \tilde{\mathbf{E}}_{-i}^H \tilde{\varepsilon}_i},$$

and with the Sherman-Morrison-Woodbury formula [12, Equation (0.7.4.1)]

$$(109) \quad \begin{aligned} \{(\zeta^2 \mathbf{I} - \tilde{\mathbf{E}}^H \tilde{\mathbf{E}})^{-1}\}_{-ii} &= (\zeta^2 \mathbf{I} - \tilde{\mathbf{E}}_{-i}^H \tilde{\mathbf{E}}_{-i})^{-1} \\ &+ \frac{(\zeta^2 \mathbf{I} - \tilde{\mathbf{E}}_{-i}^H \tilde{\mathbf{E}}_{-i})^{-1} \tilde{\mathbf{E}}_{-i}^H \tilde{\varepsilon}_i \tilde{\varepsilon}_i^H \tilde{\mathbf{E}}_{-i} (\zeta^2 \mathbf{I} - \tilde{\mathbf{E}}_{-i}^H \tilde{\mathbf{E}}_{-i})^{-1}}{\zeta^2 - \tilde{\varepsilon}_i^H \tilde{\varepsilon}_i - \tilde{\varepsilon}_i^H \tilde{\mathbf{E}}_{-i} (\zeta^2 \mathbf{I} - \tilde{\mathbf{E}}_{-i}^H \tilde{\mathbf{E}}_{-i})^{-1} \tilde{\mathbf{E}}_{-i}^H \tilde{\varepsilon}_i}, \end{aligned}$$

where $\tilde{\varepsilon}_i$ is the i th column of $\tilde{\mathbf{E}}$ and $\tilde{\mathbf{E}}_{-i}$ is $\tilde{\mathbf{E}}$ with the i th column removed. As a result,

$$(110) \quad \operatorname{tr} \mathbf{\Delta}_1(\zeta) = \zeta \left\{ \operatorname{tr} \mathbf{\Omega}_{-i} (\zeta^2 \mathbf{I} - \tilde{\mathbf{E}}_{-i}^H \tilde{\mathbf{E}}_{-i})^{-1} \mathbf{\Omega}_{-i}^H + \tilde{\gamma}_i \right\},$$

where

$$(111) \quad \tilde{\gamma}_i := \frac{\delta_i + \tilde{\varepsilon}_i^H \tilde{\mathbf{E}}_{-i} (\zeta^2 \mathbf{I} - \tilde{\mathbf{E}}_{-i}^H \tilde{\mathbf{E}}_{-i})^{-1} \mathbf{\Omega}_{-i}^H \mathbf{\Omega}_{-i} (\zeta^2 \mathbf{I} - \tilde{\mathbf{E}}_{-i}^H \tilde{\mathbf{E}}_{-i})^{-1} \tilde{\mathbf{E}}_{-i}^H \tilde{\varepsilon}_i}{\zeta^2 - \tilde{\varepsilon}_i^H \tilde{\varepsilon}_i - \tilde{\varepsilon}_i^H \tilde{\mathbf{E}}_{-i} (\zeta^2 \mathbf{I} - \tilde{\mathbf{E}}_{-i}^H \tilde{\mathbf{E}}_{-i})^{-1} \tilde{\mathbf{E}}_{-i}^H \tilde{\varepsilon}_i}.$$

Since $\text{tr } \mathbf{\Omega}_{-i}(\zeta^2 \mathbf{I} - \tilde{\mathbf{E}}_{-i}^H \tilde{\mathbf{E}}_{-i})^{-1} \mathbf{\Omega}_{-i}^H$ does not depend on $\tilde{\varepsilon}_i$,

$$(\mathbb{E}_{i-1} - \mathbb{E}_i) \left\{ \text{tr } \mathbf{\Omega}_{-i}(\zeta^2 \mathbf{I} - \tilde{\mathbf{E}}_{-i}^H \tilde{\mathbf{E}}_{-i})^{-1} \mathbf{\Omega}_{-i}^H \right\} = 0,$$

and so

$$(112) \quad \gamma_i = (\mathbb{E}_{i-1} - \mathbb{E}_i) \left\{ \frac{1}{n_1} \text{tr } \mathbf{\Delta}_1(\zeta) \right\} = \frac{\zeta}{n_1} (\mathbb{E}_{i-1} - \mathbb{E}_i)(\tilde{\gamma}_i).$$

We now bound the magnitude of $\tilde{\gamma}_i$ by observing first that

$$(113) \quad \begin{aligned} & |\tilde{\varepsilon}_i^H \tilde{\mathbf{E}}_{-i}(\zeta^2 \mathbf{I} - \tilde{\mathbf{E}}_{-i}^H \tilde{\mathbf{E}}_{-i})^{-1} \mathbf{\Omega}_{-i}^H \mathbf{\Omega}_{-i}(\zeta^2 \mathbf{I} - \tilde{\mathbf{E}}_{-i}^H \tilde{\mathbf{E}}_{-i})^{-1} \tilde{\mathbf{E}}_{-i}^H \tilde{\varepsilon}_i| \\ & \leq \| \{ (\zeta^2 \mathbf{I} - \tilde{\mathbf{E}}_{-i}^H \tilde{\mathbf{E}}_{-i})^H \}^{-1} \tilde{\mathbf{E}}_{-i}^H \tilde{\varepsilon}_i \|_2 \| (\zeta^2 \mathbf{I} - \tilde{\mathbf{E}}_{-i}^H \tilde{\mathbf{E}}_{-i})^{-1} \tilde{\mathbf{E}}_{-i}^H \tilde{\varepsilon}_i \|_2 \\ & = \| (\zeta^2 \mathbf{I} - \tilde{\mathbf{E}}_{-i}^H \tilde{\mathbf{E}}_{-i})^{-1} \tilde{\mathbf{E}}_{-i}^H \tilde{\varepsilon}_i \|_2^2, \end{aligned}$$

where the inequality follows by Cauchy-Schwarz and $\| \mathbf{\Omega}_{-i}^H \mathbf{\Omega}_{-i} \| = 1$, and the equality holds because $\zeta^2 \mathbf{I} - \tilde{\mathbf{E}}_{-i}^H \tilde{\mathbf{E}}_{-i}$ is a normal matrix even though it is *not* Hermitian. On the other hand

$$(114) \quad \begin{aligned} & \left| \zeta^2 - \tilde{\varepsilon}_i^H \tilde{\varepsilon}_i - \tilde{\varepsilon}_i^H \tilde{\mathbf{E}}_{-i}(\zeta^2 \mathbf{I} - \tilde{\mathbf{E}}_{-i}^H \tilde{\mathbf{E}}_{-i})^{-1} \tilde{\mathbf{E}}_{-i}^H \tilde{\varepsilon}_i \right| \\ & \geq \left| \Im \{ \zeta^2 - \tilde{\varepsilon}_i^H \tilde{\varepsilon}_i - \tilde{\varepsilon}_i^H \tilde{\mathbf{E}}_{-i}(\zeta^2 \mathbf{I} - \tilde{\mathbf{E}}_{-i}^H \tilde{\mathbf{E}}_{-i})^{-1} \tilde{\mathbf{E}}_{-i}^H \tilde{\varepsilon}_i \} \right| \\ & = \left| \Im(\zeta^2) + \Im(\zeta^2) \| (\zeta^2 \mathbf{I} - \tilde{\mathbf{E}}_{-i}^H \tilde{\mathbf{E}}_{-i})^{-1} \tilde{\mathbf{E}}_{-i}^H \tilde{\varepsilon}_i \|_2^2 \right| \\ & = \left| \Im(\zeta^2) \right| \left\{ 1 + \| (\zeta^2 \mathbf{I} - \tilde{\mathbf{E}}_{-i}^H \tilde{\mathbf{E}}_{-i})^{-1} \tilde{\mathbf{E}}_{-i}^H \tilde{\varepsilon}_i \|_2^2 \right\}, \end{aligned}$$

where the first equality follows by applying [3, Equation (A.1.11)] to the term $(\zeta^2 \mathbf{I} - \tilde{\mathbf{E}}_{-i}^H \tilde{\mathbf{E}}_{-i})^{-1}$ to obtain

$$\Im \{ \tilde{\varepsilon}_i^H \tilde{\mathbf{E}}_{-i}(\zeta^2 \mathbf{I} - \tilde{\mathbf{E}}_{-i}^H \tilde{\mathbf{E}}_{-i})^{-1} \tilde{\mathbf{E}}_{-i}^H \tilde{\varepsilon}_i \} = -\Im(\zeta^2) \| (\zeta^2 \mathbf{I} - \tilde{\mathbf{E}}_{-i}^H \tilde{\mathbf{E}}_{-i})^{-1} \tilde{\mathbf{E}}_{-i}^H \tilde{\varepsilon}_i \|_2^2.$$

Applying (113) and (114) to (111), and observing that $|\delta_i| \leq 1$, yields

$$(115) \quad |\tilde{\gamma}_i| \leq \frac{1 + \| (\zeta^2 \mathbf{I} - \tilde{\mathbf{E}}_{-i}^H \tilde{\mathbf{E}}_{-i})^{-1} \tilde{\mathbf{E}}_{-i}^H \tilde{\varepsilon}_i \|_2^2}{\left| \Im(\zeta^2) \right| \left\{ 1 + \| (\zeta^2 \mathbf{I} - \tilde{\mathbf{E}}_{-i}^H \tilde{\mathbf{E}}_{-i})^{-1} \tilde{\mathbf{E}}_{-i}^H \tilde{\varepsilon}_i \|_2^2 \right\}} = \frac{1}{\left| \Im(\zeta^2) \right|} = \frac{1}{2|rs|}.$$

As a result $\gamma_1, \dots, \gamma_n$ are bounded and form a complex martingale difference sequence, and applying the extended Burkholder inequality [3, Lemma 2.12] for the fourth moment yields

$$(116) \quad \begin{aligned} & \mathbb{E} \left| \frac{1}{n_1} \text{tr } \mathbf{\Delta}_1(\zeta) - \mathbb{E} \frac{1}{n_1} \text{tr } \mathbf{\Delta}_1(\zeta) \right|^4 = \mathbb{E} \left| \sum_{i=1}^n \gamma_i \right|^4 \\ & \leq K_4 \mathbb{E} \left(\sum_{i=1}^n |\gamma_i|^2 \right)^2 = K_4 \frac{|\zeta|^4}{n_1^4} \mathbb{E} \left\{ \sum_{i=1}^n |(\mathbb{E}_{i-1} - \mathbb{E}_i)(\tilde{\gamma}_i)|^2 \right\}^2 \\ & \leq K_4 \frac{|\zeta|^4}{n_1^4} \mathbb{E} \left(\sum_{i=1}^n \frac{1}{|rs|^2} \right)^2 = K_4 \frac{|\zeta|^4}{|rs|^4} \frac{n^2}{n_1^4}, \end{aligned}$$

where the final inequality follows from (115) and the fact that

$$|(\mathbb{E}_{i-1} - \mathbb{E}_i)(\tilde{\gamma}_i)| \leq |\mathbb{E}_{i-1}(\tilde{\gamma}_i)| + |\mathbb{E}_i(\tilde{\gamma}_i)| \leq \mathbb{E}_{i-1}|\tilde{\gamma}_i| + \mathbb{E}_i|\tilde{\gamma}_i|.$$

Applying the Borel-Cantelli lemma [10, Example 14.14] and recalling that $n_1/n \rightarrow p_1$ yields (104).

B.2. Pointwise convergence of the mean. Let $\zeta = r + \imath s \in \mathbb{C}$ with $r, s \neq 0$, and note that

$$(117) \quad \mathbb{E} \frac{1}{n_1} \operatorname{tr} \mathbf{\Delta}_1(\zeta) = \frac{1}{n_1} \sum_{i=1}^{n_1} \mathbb{E} \{ \zeta (\zeta^2 \mathbf{I} - \tilde{\mathbf{E}}^H \tilde{\mathbf{E}})^{-1} \}_{ii} = \frac{1}{n_1} \sum_{i=1}^{n_1} \mathbb{E} \left\{ \frac{1}{\zeta - \tilde{\varepsilon}_i^H(\zeta \mathbf{\Gamma}_i) \tilde{\varepsilon}_i} \right\},$$

where $\mathbf{\Gamma}_i := (\zeta^2 \mathbf{I} - \tilde{\mathbf{E}}_{-i} \tilde{\mathbf{E}}_{-i}^H)^{-1}$ and the expression for $\{ \zeta (\zeta^2 \mathbf{I} - \tilde{\mathbf{E}}^H \tilde{\mathbf{E}})^{-1} \}_{ii}$ comes from applying the Sherman-Morrison-Woodbury formula [12, Equation (0.7.4.1)] to the denominator in (108). Hence

$$(118) \quad \mathbb{E} \frac{1}{n_1} \operatorname{tr} \mathbf{\Delta}_1(\zeta) - \frac{1}{\mu} = \frac{1}{n_1} \sum_{i=1}^{n_1} \mathbb{E} \left(\frac{1}{\mu - \xi_i} - \frac{1}{\mu} \right) = \frac{1}{n_1} \sum_{i=1}^{n_1} \mathbb{E} \left\{ \frac{\xi_i}{\mu(\mu - \xi_i)} \right\},$$

where

$$(119) \quad \mu := \zeta - w_1^2 \sigma_1^2 \mathbb{E} \frac{1}{n} \operatorname{tr}(\zeta \mathbf{\Gamma}), \quad \xi_i := \tilde{\varepsilon}_i^H(\zeta \mathbf{\Gamma}_i) \tilde{\varepsilon}_i - w_1^2 \sigma_1^2 \mathbb{E} \frac{1}{n} \operatorname{tr}(\zeta \mathbf{\Gamma}),$$

and $\mathbf{\Gamma} := (\zeta^2 \mathbf{I} - \tilde{\mathbf{E}} \tilde{\mathbf{E}}^H)^{-1}$. Now note that

$$(120) \quad \frac{\xi_i}{\mu(\mu - \xi_i)} = \frac{\xi_i}{\mu(\mu - \xi_i)} \frac{(\mu - \xi_i) + \xi_i}{\mu} = \frac{\xi_i}{\mu^2} + \frac{\xi_i^2}{\mu^2(\mu - \xi_i)},$$

and so

$$(121) \quad \left| \mathbb{E} \left\{ \frac{\xi_i}{\mu(\mu - \xi_i)} \right\} \right| \leq \frac{|\mathbb{E}(\xi_i)|}{|\mu|^2} + \mathbb{E} \left(\frac{|\xi_i|^2}{|\mu|^2 |\mu - \xi_i|} \right).$$

For any $\lambda \in \mathbb{R}$,

$$(122) \quad \frac{\zeta}{\zeta^2 - \lambda} = \frac{\zeta((\zeta^*)^2 - \lambda)}{|\zeta^2 - \lambda|^2} = \frac{\zeta^* |\zeta|^2 - \zeta \lambda}{|\zeta^2 - \lambda|^2} = r \frac{|\zeta|^2 - \lambda}{|\zeta^2 - \lambda|^2} - \imath s \frac{|\zeta|^2 + \lambda}{|\zeta^2 - \lambda|^2},$$

and so

$$(123) \quad \begin{aligned} \operatorname{sign}[\Im\{\operatorname{tr}(\zeta \mathbf{\Gamma})\}] &= \operatorname{sign} \left[\sum_{j=1}^d \Im \left\{ \frac{\zeta}{\zeta^2 - \lambda_j(\tilde{\mathbf{E}} \tilde{\mathbf{E}}^H)} \right\} \right] \\ &= \operatorname{sign} \left[\sum_{j=1}^d \underbrace{\left\{ -s \frac{|\zeta|^2 + \lambda_j(\tilde{\mathbf{E}} \tilde{\mathbf{E}}^H)}{|\zeta^2 - \lambda_j(\tilde{\mathbf{E}} \tilde{\mathbf{E}}^H)|^2} \right\}}_{>0} \right] = -\operatorname{sign}(s), \end{aligned}$$

where sign denotes the sign of its argument, λ_j denotes the j th eigenvalue of its argument, and we use the fact that $\tilde{\mathbf{E}}\tilde{\mathbf{E}}^H$ has nonnegative eigenvalues. Hence $|\mu|$ is lower bounded as

$$(124) \quad |\mu| \geq \left| \Im \left\{ \zeta - w_1^2 \sigma_1^2 \mathbb{E} \frac{1}{n} \text{tr}(\zeta \mathbf{\Gamma}) \right\} \right| = \left| s - w_1^2 \sigma_1^2 \mathbb{E} \frac{1}{n} \Im \{ \text{tr}(\zeta \mathbf{\Gamma}) \} \right| \geq |s|.$$

Likewise, $\text{sign}[\Im\{\tilde{\varepsilon}_i^H(\zeta \mathbf{\Gamma}_i)\tilde{\varepsilon}_i\}] = -\text{sign}(s)$ and $|\mu - \xi_i| \geq |s|$. As a result, (121) is further bounded as

$$(125) \quad \left| \mathbb{E} \left\{ \frac{\xi_i}{\mu(\mu - \xi_i)} \right\} \right| \leq \frac{|\mathbb{E}(\xi_i)|}{|s|^2} + \frac{\mathbb{E}|\xi_i|^2}{|s|^3} = \frac{|\mathbb{E}(\xi_i)|}{|s|^2} + \frac{|\mathbb{E}(\xi_i)|^2}{|s|^3} + \frac{\mathbb{E}|\xi_i - \mathbb{E}(\xi_i)|^2}{|s|^3},$$

so it remains to bound the mean and variance of ξ_i . Note that

$$(126) \quad |\mathbb{E}(\xi_i)| = \left| w_1^2 \sigma_1^2 \mathbb{E} \frac{1}{n} \text{tr}(\zeta \mathbf{\Gamma}_i) - w_1^2 \sigma_1^2 \mathbb{E} \frac{1}{n} \text{tr}(\zeta \mathbf{\Gamma}) \right| \leq \frac{w_1^2 \sigma_1^2}{n} \mathbb{E} |\text{tr}(\zeta \mathbf{\Gamma}_i) - \text{tr}(\zeta \mathbf{\Gamma})|,$$

since $\tilde{\varepsilon}_i$ and $\mathbf{\Gamma}_i$ are independent and $\mathbb{E}(\tilde{\varepsilon}_i \tilde{\varepsilon}_i^H) = (w_1^2 \sigma_1^2 / n) \mathbf{I}$ when $i \in [1, n_1]$. Next, observe that

$$(127) \quad |\text{tr}(\zeta \mathbf{\Gamma}_i) - \text{tr}(\zeta \mathbf{\Gamma})| = |\zeta| \frac{|\tilde{\varepsilon}_i^H \mathbf{\Gamma}_i^2 \tilde{\varepsilon}_i|}{|1 - \tilde{\varepsilon}_i^H \mathbf{\Gamma}_i \tilde{\varepsilon}_i|} \leq \frac{|\zeta|}{2|rs|},$$

where the equality follows from applying the Sherman-Morrison-Woodbury formula [12, Equation (0.7.4.1)] to $\mathbf{\Gamma} = (\zeta^2 \mathbf{I} - \tilde{\mathbf{E}}_{-i} \tilde{\mathbf{E}}_{-i}^H - \tilde{\varepsilon}_i \tilde{\varepsilon}_i^H)^{-1}$ then simplifying. The inequality follows in a similar way as in [3, Section 3.3.2, Step 1]. Substituting (127) into (126) yields the bound on the mean:

$$(128) \quad |\mathbb{E}(\xi_i)| \leq \frac{w_1^2 \sigma_1^2}{n} \mathbb{E} \left(\frac{|\zeta|}{2|rs|} \right) = \frac{1}{n} \frac{w_1^2 \sigma_1^2 |\zeta|}{2|rs|}.$$

Now note that

$$(129) \quad \begin{aligned} \mathbb{E} |\xi_i - \mathbb{E}(\xi_i)|^2 &= \mathbb{E} \left| \tilde{\varepsilon}_i^H (\zeta \mathbf{\Gamma}_i) \tilde{\varepsilon}_i - w_1^2 \sigma_1^2 \mathbb{E} \frac{1}{n} \text{tr}(\zeta \mathbf{\Gamma}_i) \right|^2 \\ &= \mathbb{E} \left| \tilde{\varepsilon}_i^H (\zeta \mathbf{\Gamma}_i) \tilde{\varepsilon}_i - w_1^2 \sigma_1^2 \frac{1}{n} \text{tr}(\zeta \mathbf{\Gamma}_i) \right|^2 + w_1^4 \sigma_1^4 \mathbb{E} \left| \frac{1}{n} \text{tr}(\zeta \mathbf{\Gamma}_i) - \mathbb{E} \frac{1}{n} \text{tr}(\zeta \mathbf{\Gamma}_i) \right|^2, \end{aligned}$$

since $\mathbb{E}_{\tilde{\varepsilon}_i} \{ \tilde{\varepsilon}_i^H (\zeta \mathbf{\Gamma}_i) \tilde{\varepsilon}_i \} = w_1^2 \sigma_1^2 (1/n) \text{tr}(\zeta \mathbf{\Gamma}_i)$. Defining $\mathbf{T} := \zeta \mathbf{\Gamma}_i$ and recalling

that $\tilde{\varepsilon}_i = (w_1\sigma_1/\sqrt{n})\varepsilon_i$, the first term in (129) is

$$\begin{aligned}
(130) \quad & \frac{w_1^4\sigma_1^4}{n^2} \mathbb{E} |\varepsilon_i^H \mathbf{T} \varepsilon_i - \text{tr } \mathbf{T}|^2 = \frac{w_1^4\sigma_1^4}{n^2} \mathbb{E} \left| \sum_{p,q=1}^d \mathbf{E}_{pi}^* \mathbf{E}_{qi} \mathbf{T}_{pq} - \sum_{p=1}^d \mathbf{T}_{pp} \right|^2 \\
& = \frac{w_1^4\sigma_1^4}{n^2} \mathbb{E} \left| \sum_{p \neq q} \mathbf{E}_{pi}^* \mathbf{E}_{qi} \mathbf{T}_{pq} + \sum_{p=1}^d \mathbf{T}_{pp} (|\mathbf{E}_{pi}|^2 - 1) \right|^2 \\
& = \frac{w_1^4\sigma_1^4}{n^2} \left(\mathbb{E} \left| \sum_{p \neq q} \mathbf{E}_{pi}^* \mathbf{E}_{qi} \mathbf{T}_{pq} \right|^2 + \mathbb{E} \left| \sum_{p=1}^d \mathbf{T}_{pp} (|\mathbf{E}_{pi}|^2 - 1) \right|^2 \right. \\
& \quad \left. + 2\Re \mathbb{E} \left[\left(\sum_{p \neq q} \mathbf{E}_{pi}^* \mathbf{E}_{qi} \mathbf{T}_{pq} \right)^* \left\{ \sum_{p=1}^d \mathbf{T}_{pp} (|\mathbf{E}_{pi}|^2 - 1) \right\} \right] \right).
\end{aligned}$$

Since the entries of \mathbf{E} are independent and mean zero,

$$(131) \quad \mathbb{E} \left[\left(\sum_{p \neq q} \mathbf{E}_{pi}^* \mathbf{E}_{qi} \mathbf{T}_{pq} \right)^* \left\{ \sum_{p=1}^d \mathbf{T}_{pp} (|\mathbf{E}_{pi}|^2 - 1) \right\} \right] = 0,$$

so it remains to bound the other two terms in (130). Observe that

$$\begin{aligned}
(132) \quad & \mathbb{E} \left| \sum_{p \neq q} \mathbf{E}_{pi}^* \mathbf{E}_{qi} \mathbf{T}_{pq} \right|^2 = \sum_{\substack{p \neq q \\ j \neq k}} \mathbb{E} \left(\mathbf{E}_{pi} \mathbf{E}_{qi}^* \mathbf{T}_{pq}^* \mathbf{E}_{ji}^* \mathbf{E}_{ki} \mathbf{T}_{jk} \right) \\
& = \sum_{p \neq q} \mathbb{E} \left(\mathbf{E}_{pi} \mathbf{E}_{qi}^* \mathbf{T}_{pq}^* \mathbf{E}_{pi}^* \mathbf{E}_{qi} \mathbf{T}_{pq} \right) + \sum_{p \neq q} \mathbb{E} \left(\mathbf{E}_{pi} \mathbf{E}_{qi}^* \mathbf{T}_{pq}^* \mathbf{E}_{qi}^* \mathbf{E}_{pi} \mathbf{T}_{qp} \right) \\
& = \sum_{p \neq q} \mathbb{E} |\mathbf{E}_{pi}|^2 \mathbb{E} |\mathbf{E}_{qi}|^2 \mathbb{E} |\mathbf{T}_{pq}|^2 + \sum_{p \neq q} \mathbb{E} (\mathbf{E}_{pi})^2 \mathbb{E} (\mathbf{E}_{qi}^*)^2 \mathbb{E} (\mathbf{T}_{pq}^* \mathbf{T}_{qp}),
\end{aligned}$$

where the second equality is obtained by dropping terms in the sum with expectation equal to zero, e.g., terms with $p \neq q, j, k$ for which $\mathbb{E}(\mathbf{E}_{pi}) = 0$ can be pulled out by independence. Now note that

$$\begin{aligned}
(133) \quad & \sum_{p \neq q} \mathbb{E} (\mathbf{E}_{pi})^2 \mathbb{E} (\mathbf{E}_{qi}^*)^2 \mathbb{E} (\mathbf{T}_{pq}^* \mathbf{T}_{qp}) \leq \sum_{p \neq q} |\mathbb{E} (\mathbf{E}_{pi})^2 \mathbb{E} (\mathbf{E}_{qi}^*)^2 \mathbb{E} (\mathbf{T}_{pq}^* \mathbf{T}_{qp})| \\
& \leq \sum_{p \neq q} \mathbb{E} |\mathbf{E}_{pi}|^2 \mathbb{E} |\mathbf{E}_{qi}|^2 \mathbb{E} |\mathbf{T}_{pq}^* \mathbf{T}_{qp}| = \sum_{p \neq q} \mathbb{E} |\mathbf{T}_{pq}^* \mathbf{T}_{qp}| \leq \sum_{p \neq q} \mathbb{E} |\mathbf{T}_{pq}|^2,
\end{aligned}$$

where the second inequality follows from Jensen's inequality, the equality holds because $\mathbb{E} |\mathbf{E}_{pi}|^2 = \mathbb{E} |\mathbf{E}_{qi}|^2 = 1$, and the final inequality follows from

the arithmetic mean geometric mean inequality as

$$\begin{aligned} \sum_{p \neq q} \mathbb{E} |\mathbf{T}_{pq}^* \mathbf{T}_{qp}| &= \sum_{p \neq q} \mathbb{E} (|\mathbf{T}_{pq}| |\mathbf{T}_{qp}|) = \sum_{p \neq q} \mathbb{E} \left(\sqrt{|\mathbf{T}_{pq}|^2 |\mathbf{T}_{qp}|^2} \right) \\ &\leq \sum_{p \neq q} \mathbb{E} \left(\frac{|\mathbf{T}_{pq}|^2 + |\mathbf{T}_{qp}|^2}{2} \right) = \sum_{p \neq q} \mathbb{E} |\mathbf{T}_{pq}|^2. \end{aligned}$$

Combining (132) and (133), and recalling that $\mathbb{E} |\mathbf{E}_{pi}|^2 = 1$, yields

$$(134) \quad \mathbb{E} \left| \sum_{p \neq q} \mathbf{E}_{pi}^* \mathbf{E}_{qi} \mathbf{T}_{pq} \right|^2 \leq 2 \sum_{p \neq q} \mathbb{E} |\mathbf{T}_{pq}|^2 \leq 2 \sum_{p, q=1}^d \mathbb{E} |\mathbf{T}_{pq}|^2.$$

Denoting $\kappa > 1$ for an upper bound to $\mathbb{E} |\mathbf{E}_{pi}|^4 < \infty$, the second term in (130) is bounded as

$$(135) \quad \begin{aligned} \mathbb{E} \left| \sum_{p=1}^d \mathbf{T}_{pp} (|\mathbf{E}_{pi}|^2 - 1) \right|^2 &= \sum_{p=1}^d \mathbb{E} |\mathbf{T}_{pp}|^2 (\mathbb{E} |\mathbf{E}_{pi}|^4 - 1) \\ &\leq (\kappa - 1) \sum_{p=1}^d \mathbb{E} |\mathbf{T}_{pp}|^2 \leq (\kappa - 1) \sum_{p, q=1}^d \mathbb{E} |\mathbf{T}_{pq}|^2. \end{aligned}$$

where the equality can be obtained by expanding the squared magnitude and dropping terms from the resulting double sum that are equal to zero.

Combining (131), (134), and (135) yields the bound for (130),

$$(136) \quad \begin{aligned} \frac{w_1^4 \sigma_1^4}{n^2} \mathbb{E} |\varepsilon_i^H \mathbf{T} \varepsilon_i - \text{tr} \mathbf{T}|^2 &\leq \frac{w_1^4 \sigma_1^4}{n^2} \left\{ 2 \sum_{p, q=1}^d \mathbb{E} |\mathbf{T}_{pq}|^2 + (\kappa - 1) \sum_{p, q=1}^d \mathbb{E} |\mathbf{T}_{pq}|^2 \right\} \\ &= \frac{w_1^4 \sigma_1^4}{n^2} (\kappa + 1) \sum_{p, q=1}^d \mathbb{E} |\mathbf{T}_{pq}|^2 \leq \frac{w_1^4 \sigma_1^4}{n^2} (\kappa + 1) \frac{d |\zeta|^2}{4 |rs|^2} = \frac{d}{n^2} \frac{w_1^4 \sigma_1^4 (\kappa + 1) |\zeta|^2}{4 |rs|^2}, \end{aligned}$$

where the final inequality holds because

$$\begin{aligned} \sum_{p, q=1}^d \mathbb{E} |\mathbf{T}_{pq}|^2 &= \mathbb{E} \text{tr}(\mathbf{T} \mathbf{T}^H) = \mathbb{E} \left\{ \sum_{j=1}^d \frac{|\zeta|^2}{|\zeta^2 - \lambda_j(\tilde{\mathbf{E}}_{-j} \tilde{\mathbf{E}}_{-j}^H)|^2} \right\} \\ &\leq \mathbb{E} \left\{ \sum_{j=1}^d \frac{|\zeta|^2}{|\Im\{\zeta^2 - \lambda_j(\tilde{\mathbf{E}}_{-j} \tilde{\mathbf{E}}_{-j}^H)\}|^2} \right\} = \mathbb{E} \left\{ \sum_{j=1}^d \frac{|\zeta|^2}{(2|rs|)^2} \right\} = \frac{d |\zeta|^2}{4 |rs|^2}, \end{aligned}$$

where λ_j denotes the j th eigenvalue of its argument.

To bound the second term in (129), consider the expansion

$$(137) \quad \frac{1}{n} \operatorname{tr}(\zeta \mathbf{\Gamma}_i) - \mathbb{E} \frac{1}{n} \operatorname{tr}(\zeta \mathbf{\Gamma}_i) = \sum_{j=1}^n \underbrace{(\mathbb{E}_{j-1} - \mathbb{E}_j)}_{=: \nu_j} \left\{ \frac{1}{n} \operatorname{tr}(\zeta \mathbf{\Gamma}_i) \right\},$$

where \mathbb{E}_j denotes expectation over the first j columns of $\tilde{\mathbf{E}}$. Note that $\nu_i = 0$ since $(1/n) \operatorname{tr}(\zeta \mathbf{\Gamma}_i)$ does not involve $\tilde{\varepsilon}_i$. When $j \neq i$

$$(138) \quad \begin{aligned} |\nu_j| &= \frac{1}{n} \left| (\mathbb{E}_{j-1} - \mathbb{E}_j) \left[\operatorname{tr} \{ \zeta (\zeta^2 \mathbf{I} - \tilde{\mathbf{E}}_{-i} \tilde{\mathbf{E}}_{-i}^{\mathbf{H}})^{-1} \} \right. \right. \\ &\quad \left. \left. - \operatorname{tr} \{ \zeta (\zeta^2 \mathbf{I} - \tilde{\mathbf{E}}_{-i,j} \tilde{\mathbf{E}}_{-i,j}^{\mathbf{H}})^{-1} \} \right] \right| \\ &\leq \frac{1}{n} (\mathbb{E}_{j-1} + \mathbb{E}_j) \left| \operatorname{tr} \{ \zeta (\zeta^2 \mathbf{I} - \tilde{\mathbf{E}}_{-i} \tilde{\mathbf{E}}_{-i}^{\mathbf{H}})^{-1} \} \right. \\ &\quad \left. - \operatorname{tr} \{ \zeta (\zeta^2 \mathbf{I} - \tilde{\mathbf{E}}_{-i,j} \tilde{\mathbf{E}}_{-i,j}^{\mathbf{H}})^{-1} \} \right| \\ &\leq \frac{1}{n} (\mathbb{E}_{j-1} + \mathbb{E}_j) \frac{|\zeta|}{2|rs|} = \frac{1}{n} \frac{|\zeta|}{|rs|}, \end{aligned}$$

where $\tilde{\mathbf{E}}_{-i,j}$ is $\tilde{\mathbf{E}}$ with both the i th and the j th columns removed, and the final inequality follows in a similar way as (127). As a result ν_1, \dots, ν_n form a complex martingale difference sequence, and applying the extended Burkholder inequality [3, Lemma 2.12] for the second moment yields

$$(139) \quad \begin{aligned} \mathbb{E} \left| \frac{1}{n} \operatorname{tr}(\zeta \mathbf{\Gamma}_i) - \mathbb{E} \frac{1}{n} \operatorname{tr}(\zeta \mathbf{\Gamma}_i) \right|^2 &= \mathbb{E} \left| \sum_{j=1}^n \nu_j \right|^2 \\ &\leq K_2 \mathbb{E} \sum_{j=1}^n |\nu_j|^2 \leq K_2 \mathbb{E} \sum_{j=1}^n \frac{1}{n^2} \frac{|\zeta|^2}{|rs|^2} = \frac{1}{n} \frac{K_2 |\zeta|^2}{|rs|^2}. \end{aligned}$$

Substituting (136) and (139) into (129) yields the variance bound for ξ_i :

$$(140) \quad \mathbb{E} |\xi_i - \mathbb{E}(\xi_i)|^2 \leq \frac{d}{n^2} \frac{w_1^4 \sigma_1^4 (\kappa + 1) |\zeta|^2}{4|rs|^2} + \frac{1}{n} \frac{w_1^4 \sigma_1^4 K_2 |\zeta|^2}{|rs|^2}.$$

Finally, combining (118), (125), (128), and (140) yields

$$\begin{aligned}
(141) \quad & \left| \mathbb{E} \frac{1}{n_1} \operatorname{tr} \mathbf{\Delta}_1(\zeta) - \frac{1}{\mu} \right| \leq \frac{1}{n_1} \sum_{i=1}^{n_1} \left| \mathbb{E} \left\{ \frac{\xi_i}{\mu(\mu - \xi_i)} \right\} \right| \\
& \leq \frac{1}{n_1} \sum_{i=1}^{n_1} \left(\frac{1}{n} \frac{w_1^2 \sigma_1^2 |\zeta|}{2|r s^3|} + \frac{1}{n^2} \frac{w_1^4 \sigma_1^4 |\zeta|^2}{4|r^2 s^5|} \right. \\
& \quad \left. + \frac{d}{n^2} \frac{w_1^4 \sigma_1^4 (\kappa + 1) |\zeta|^2}{4|r^2 s^5|} + \frac{1}{n} \frac{w_1^4 \sigma_1^4 K_2 |\zeta|^2}{|r^2 s^5|} \right) \\
& = \frac{1}{n} \left(\frac{w_1^2 \sigma_1^2 |\zeta|}{2|r s^3|} + \frac{w_1^4 \sigma_1^4 K_2 |\zeta|^2}{|r^2 s^5|} \right) + \frac{1}{n^2} \frac{w_1^4 \sigma_1^4 |\zeta|^2}{4|r^2 s^5|} + \frac{d}{n^2} \frac{w_1^4 \sigma_1^4 (\kappa + 1) |\zeta|^2}{4|r^2 s^5|} \\
& \rightarrow 0,
\end{aligned}$$

since $1/n, 1/n^2, d/n^2 \rightarrow 0$ as $n, d \rightarrow \infty$ while $n/d \rightarrow c$, and (105) follows by observing that

$$\mathbb{E} \frac{1}{n} \operatorname{tr}(\zeta \mathbf{\Gamma}) = \frac{d}{n} \mathbb{E} \frac{1}{d} \operatorname{tr} \{ \zeta (\zeta^2 \mathbf{I} - \tilde{\mathbf{E}} \tilde{\mathbf{E}}^H)^{-1} \} \rightarrow \frac{\varphi_1(\zeta)}{c},$$

and $|\mu|, |\zeta - w_1^2 \sigma_1^2 \varphi_1(\zeta)/c| \geq |s| \neq 0$.

B.3. Almost sure uniform convergence. Let $\tau > 0$ be arbitrary, and consider the (countable) set

$$(142) \quad \mathbb{C}_0 := \{r + is : r \in \mathbb{Q}, s \in \mathbb{Q}, r > b + \tau, s \neq 0\} \subset \{\zeta \in \mathbb{C} : \Re(\zeta) > b + \tau\},$$

and observe that for any $\zeta \in \mathbb{C}_0$ it follows from (103)–(105) that

$$(143) \quad \frac{1}{n} \operatorname{tr} \zeta \mathbf{W} (\zeta^2 \mathbf{I} - \tilde{\mathbf{E}}^H \tilde{\mathbf{E}})^{-1} \mathbf{W} \xrightarrow{\text{a.s.}} \sum_{\ell=1}^L \frac{p_\ell w_\ell^2}{\zeta - \tilde{\sigma}_\ell^2 \varphi_1(\zeta)/c}.$$

More precisely

$$(144) \quad \forall \zeta \in \mathbb{C}_0 \quad \Pr \left\{ \frac{1}{n} \operatorname{tr} \zeta \mathbf{W} (\zeta^2 \mathbf{I} - \tilde{\mathbf{E}}^H \tilde{\mathbf{E}})^{-1} \mathbf{W} \rightarrow \sum_{\ell=1}^L \frac{p_\ell w_\ell^2}{\zeta - \tilde{\sigma}_\ell^2 \varphi_1(\zeta)/c} \right\} = 1,$$

but since \mathbb{C}_0 is countable, it follows that

$$(145) \quad \Pr \left\{ \forall \zeta \in \mathbb{C}_0 \quad \frac{1}{n} \operatorname{tr} \zeta \mathbf{W} (\zeta^2 \mathbf{I} - \tilde{\mathbf{E}}^H \tilde{\mathbf{E}})^{-1} \mathbf{W} \rightarrow \sum_{\ell=1}^L \frac{p_\ell w_\ell^2}{\zeta - \tilde{\sigma}_\ell^2 \varphi_1(\zeta)/c} \right\} = 1.$$

Now consider $\zeta \in \mathbb{C}$ with $\Re(\zeta) > b + \tau$, and observe that eventually $\Re(\zeta)$ for all such ζ exceed all the singular values of $\tilde{\mathbf{E}}$ by at least $\tau/2$ since the largest singular value of $\tilde{\mathbf{E}}$ converges to b . Thus, eventually

$$(146) \quad \left| \frac{1}{n} \text{tr} \zeta \mathbf{W} (\zeta^2 \mathbf{I} - \tilde{\mathbf{E}}^H \tilde{\mathbf{E}})^{-1} \mathbf{W} \right|^2 = \left| \frac{1}{n} \text{tr} \{ \mathbf{W}^2 \zeta (\zeta^2 \mathbf{I} - \tilde{\mathbf{E}}^H \tilde{\mathbf{E}})^{-1} \} \right|^2 \\ \leq \left(\frac{1}{n} \|\mathbf{W}^2\|_F^2 \right) \left\{ \frac{1}{n} \|\zeta (\zeta^2 \mathbf{I} - \tilde{\mathbf{E}}^H \tilde{\mathbf{E}})^{-1}\|_F^2 \right\} \leq \frac{4}{\tau^2} \sum_{\ell=1}^L p_\ell w_\ell^4,$$

where the first inequality follows from the Cauchy-Schwarz inequality, and the second inequality holds because $\|\mathbf{W}^2\|_F^2/n = p_1 w_1^4 + \dots + p_L w_L^4$ and

$$(147) \quad \frac{1}{n} \|\zeta (\zeta^2 \mathbf{I} - \tilde{\mathbf{E}}^H \tilde{\mathbf{E}})^{-1}\|_F^2 \\ = \frac{1}{n} \sum_{j=1}^n \left| \frac{\zeta}{\zeta^2 - \nu_j^2(\tilde{\mathbf{E}})} \right|^2 = \frac{1}{n} \sum_{j=1}^n \left\{ \frac{1}{|\zeta - \nu_j(\tilde{\mathbf{E}})|} \frac{|\zeta|}{|\zeta + \nu_j(\tilde{\mathbf{E}})|} \right\}^2 \\ \leq \frac{1}{n} \sum_{j=1}^n \frac{1}{|\zeta - \nu_j(\tilde{\mathbf{E}})|^2} \leq \frac{1}{n} \sum_{j=1}^n \frac{1}{|\Re(\zeta) - \nu_j(\tilde{\mathbf{E}})|^2} \leq \frac{4}{\tau^2}$$

where ν_j denotes the j th largest singular value of its argument, and we use the fact that $\Re(\zeta), \nu_j(\tilde{\mathbf{E}}) \geq 0$. Applying [3, Lemma 2.14] yields, almost surely, the uniform convergence (25) and the derivative convergence (27).

B.4. Properties. This section concludes the proof by verifying the following properties (26) of φ_2 :

- a) For any $\zeta > b$, almost surely eventually ζ^2 exceeds all the square singular values of $\tilde{\mathbf{E}}$, so $(\zeta^2 \mathbf{I} - \tilde{\mathbf{E}}^H \tilde{\mathbf{E}})^{-1} \succeq (1/\zeta^2) \mathbf{I}$ and

$$(148) \quad \frac{1}{n} \text{tr} \zeta \mathbf{W} (\zeta^2 \mathbf{I} - \tilde{\mathbf{E}}^H \tilde{\mathbf{E}})^{-1} \mathbf{W} \geq \frac{1}{\zeta} \sum_{\ell=1}^L \frac{n_\ell}{n} w_\ell^2 > 0.$$

Thus $\varphi_2(\zeta) > 0$ for all $\zeta > b$.

- b) As $|\zeta| \rightarrow \infty$, $|\zeta - w_\ell^2 \sigma_\ell^2 \varphi_1(\zeta)/c| \rightarrow \infty$ for each $\ell \in \{1, \dots, L\}$ since $\varphi_1(\zeta) \rightarrow 0$ as shown in Appendix A.1. Thus $\varphi_2(\zeta) \rightarrow 0$ as $|\zeta| \rightarrow \infty$.
c) As shown in Appendix A.1, $\Im\{\varphi_1(\zeta)\}$ is zero if $\Im(\zeta)$ is zero and has the opposite sign of $\Im(\zeta)$ otherwise. As a result,

$$\Im\{\zeta - w_\ell^2 \sigma_\ell^2 \varphi_1(\zeta)/c\} = \Im(\zeta) - (w_\ell^2 \sigma_\ell^2/c) \Im\{\varphi_1(\zeta)\}$$

is zero if $\Im(\zeta)$ is zero and has the same sign as $\Im(\zeta)$ otherwise. Thus we conclude that $\varphi_2(\zeta) \in \mathbb{R} \Leftrightarrow \zeta \in \mathbb{R}$.

APPENDIX C: PROOF OF LEMMA 8

Let $Q \subset P$ be the set of points that maximize f , and note that it is nonempty by assumption. Since every level set of f is a flat, there exists some matrix A and vector b such that

$$(149) \quad Q = P \cap \{x \in \mathbb{R}^n : Ax = b\},$$

so Q is also a polyhedron. Since P has at least one extreme point, Q must also have at least one extreme point.

Let x be an extreme point of Q . Next we show that x is an extreme point of P by contradiction. Suppose x is not an extreme point of P . Then there exist points $y, z \in P$, both different from x , that have convex combination equal to x . Without loss of generality, let $f(y) \leq f(z)$. Recalling that $x \in Q$ maximizes f yields

$$(150) \quad f(y) \leq f(z) \leq f(x).$$

By the intermediate value theorem, there exists some \tilde{z} between y and x for which $f(\tilde{z}) = f(z)$. Namely, z and \tilde{z} lie in the same level set, as do their affine combinations because the level sets are flats. In particular, both y and x are affine combinations of z and \tilde{z} , and as a result

$$(151) \quad f(y) = f(\tilde{z}) = f(x) = f(z),$$

and so $y, z \in Q$, implying that x is not an extreme point of Q and producing a contradiction. Thus x is an extreme point of P that maximizes f . \square

APPENDIX D: ADDITIONAL NUMERICAL SIMULATIONS

This section provides additional numerical simulations to demonstrate that the asymptotic results of Theorem 1 provide meaningful predictions for finitely many samples in finitely many dimensions. In particular, this section provides analogous plots to Fig. 9 in Section 9 for the:

- amplitudes $\hat{\theta}_i^2$ in Fig. 11,
- weighted score recoveries $|\langle \hat{z}_i/\sqrt{n}, z_i/\sqrt{n} \rangle_{\mathbf{W}_2}|^2$ in Fig. 12,
- products $\langle \hat{u}_i, u_i \rangle \langle \hat{z}_i/\sqrt{n}, z_i/\sqrt{n} \rangle_{\mathbf{W}_2}^*$ in Fig. 13.

As in Section 9, data are generated according to the model (3) with $c = 1$ sample per dimension, underlying amplitudes $\theta_1^2 = 25$ and $\theta_2^2 = 16$, and $p_1 = 20\%$ of samples having noise variance $\sigma_1^2 = 1$ with the remaining $p_2 = 80\%$ of samples having noise variance $\sigma_2^2 = 4$. Underlying scores and unscaled noise entries are both generated from the standard normal distribution, i.e.,

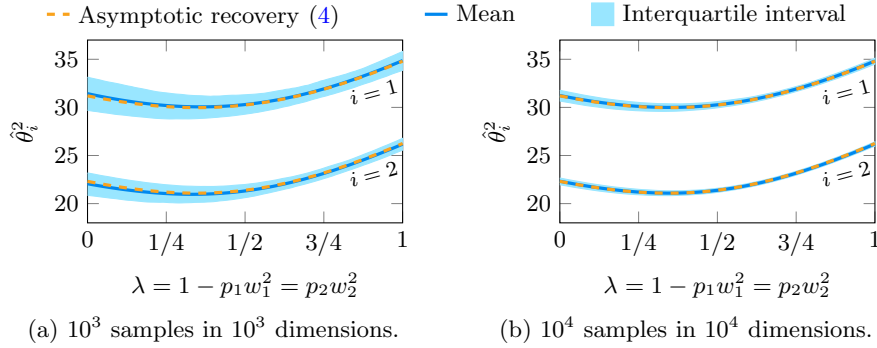


FIG 11. Simulated amplitudes $\hat{\theta}_i^2$ for data generated according to the model (3) with $c = 1$ sample per dimension, underlying amplitudes $\theta_1^2 = 25$ and $\theta_2^2 = 16$, and $p_1 = 20\%$ of samples having noise variance $\sigma_1^2 = 1$ with the remaining $p_2 = 80\%$ of samples having noise variance $\sigma_2^2 = 4$. Weights are set as $w_1^2 = (1 - \lambda)/p_1$ and $w_2^2 = \lambda/p_2$. Simulation mean (blue curve) and interquartile interval (light blue ribbon) are shown with the asymptotic prediction (4) of Theorem 1 (orange dashed curve). Increasing the data size from (a) to (b) shrinks the interquartile intervals, indicating concentration to the mean, which is itself converging to the asymptotic recovery.

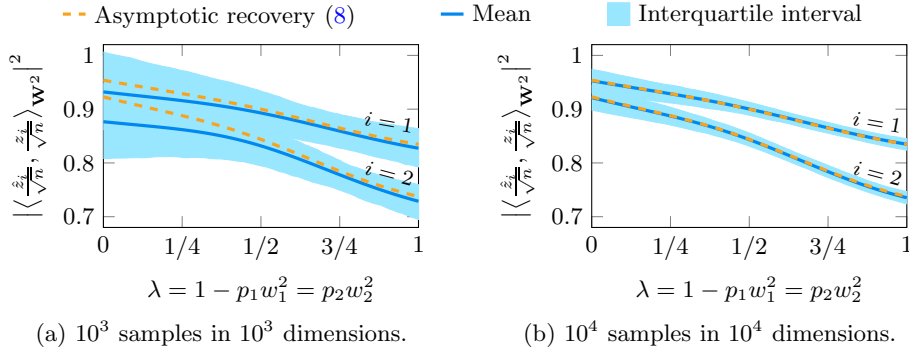


FIG 12. Simulated weighted score recoveries $|\langle \hat{z}_i/\sqrt{n}, z_i/\sqrt{n} \rangle_{\mathbf{W}^2}|^2$ for data generated according to the model (3) with $c = 1$ sample per dimension, underlying amplitudes $\theta_1^2 = 25$ and $\theta_2^2 = 16$, and $p_1 = 20\%$ of samples having noise variance $\sigma_1^2 = 1$ with the remaining $p_2 = 80\%$ of samples having noise variance $\sigma_2^2 = 4$. Weights are set as $w_1^2 = (1 - \lambda)/p_1$ and $w_2^2 = \lambda/p_2$. Simulation mean (blue curve) and interquartile interval (light blue ribbon) are shown with the asymptotic prediction (8) of Theorem 1 (orange dashed curve). Increasing the data size from (a) to (b) shrinks the interquartile intervals, indicating concentration to the mean, which is itself converging to the asymptotic recovery.

$z_{ij}, \varepsilon_{ij} \sim \mathcal{N}(0, 1)$, and the weights are set to $w_1^2 = (1 - \lambda)/p_1$ and $w_2^2 = \lambda/p_2$ where λ is swept from zero to one.

Two simulations are shown: the first has $n = 10^3$ samples in $d = 10^3$

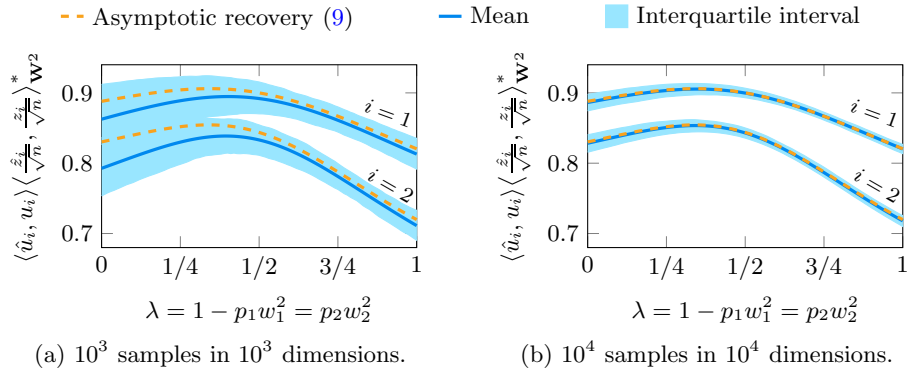


FIG 13. Simulated products $\langle \hat{u}_i, u_i \rangle \langle \hat{z}_i / \sqrt{n}, z_i / \sqrt{n} \rangle^* \mathbf{w}_2^2$ for data generated according to the model (3) with $c = 1$ sample per dimension, underlying amplitudes $\theta_1^2 = 25$ and $\theta_2^2 = 16$, and $p_1 = 20\%$ of samples having noise variance $\sigma_1^2 = 1$ with the remaining $p_2 = 80\%$ of samples having noise variance $\sigma_2^2 = 4$. Weights are set as $w_1^2 = (1 - \lambda)/p_1$ and $w_2^2 = \lambda/p_2$. Simulation mean (blue curve) and interquartile interval (light blue ribbon) are shown with the asymptotic prediction (9) of Theorem 1 (orange dashed curve). Increasing the data size from (a) to (b) shrinks the interquartile intervals, indicating concentration to the mean, which is itself converging to the asymptotic recovery.

dimensions, and the second increases these to $n = 10^4$ samples in $d = 10^4$ dimensions. Both are repeated for 500 trials. As in Fig. 9, the first simulation illustrates general agreement in behavior between the non-asymptotic recovery and its asymptotic prediction, and the second simulation shows what happens when the number of samples and dimensions are increased. The interquartile intervals shrink dramatically, indicating concentration of each recovery (a random quantity) around its mean, and each mean converges to the corresponding limit.

Acknowledgements. The authors thank Raj Rao Nadakuditi, Romain Couillet and Edgar Dobriban for helpful discussions regarding the singular values and vectors of low rank perturbations of large random matrices. The authors also thank Dejiao Zhang for helpful comments about the form of the optimal weights.

References.

- [1] ANDERSON, G., GUIONNET, A. and ZEITOUNI, O. (2009). *An introduction to random matrices* **118**. Cambridge University Press.
- [2] ARDEKANI, B. A., KERSHAW, J., KASHIKURA, K. and KANNO, I. (1999). Activation detection in functional MRI using subspace modeling and maximum likelihood estimation. *IEEE Transactions on Medical Imaging* **18**.
- [3] BAI, Z. and SILVERSTEIN, J. W. (2010). *Spectral Analysis of Large Dimensional Random Matrices*. Springer New York.

- [4] BENAYCH-GEORGES, F. and NADAKUDITI, R. R. (2012). The singular values and vectors of low rank perturbations of large rectangular random matrices. *Journal of Multivariate Analysis* **111**.
- [5] BERTSIMAS, D. and TSITSIKLIS, J. (1997). *Introduction to Linear Optimization*. Athena Scientific.
- [6] COCHRAN, R. N. and HORNE, F. H. (1977). Statistically weighted principal component analysis of rapid scanning wavelength kinetics experiments. *Analytical Chemistry* **49**.
- [7] DEVILLE, J. C. and MALINVAUD, E. (1983). Data Analysis in Official Socio-Economic Statistics. *Journal of the Royal Statistical Society. Series A (General)* **146**.
- [8] DOBRIBAN, E., LEEB, W. and SINGER, A. (2018). Optimal prediction in the linearly transformed spiked model. arXiv: 1709.03393.
- [9] GREENACRE, M. J. (1984). *Theory and Applications of Correspondence Analysis*. London (UK) Academic Press.
- [10] GUBNER, J. A. (2006). *Probability and Random Processes for Electrical and Computer Engineers*. Cambridge University Press.
- [11] HONG, D., BALZANO, L. and FESSLER, J. A. (2018). Asymptotic performance of PCA for high-dimensional heteroscedastic data. *Journal of Multivariate Analysis* **167**.
- [12] HORN, R. A. and JOHNSON, C. R. (2013). *Matrix Analysis*, 2 ed. Cambridge University Press.
- [13] JANSEN, J. J., HOEFSLOOT, H. C. J., BOELENS, H. F. M., VAN DER GREEF, J. and SMILDE, A. K. (2004). Analysis of longitudinal metabolomics data. *Bioinformatics* **20**.
- [14] JOHNSTONE, I. M. and TITTERINGTON, D. M. (2009). Statistical challenges of high-dimensional data. *Philosophical Transactions of the Royal Society A: Mathematical, Physical and Engineering Sciences* **367**.
- [15] JOLLIFFE, I. T. (2002). *Principal Component Analysis*, 2 ed. Springer-Verlag.
- [16] LEDOIT, O. and WOLF, M. (2015). Spectrum estimation: A unified framework for covariance matrix estimation and PCA in large dimensions. *Journal of Multivariate Analysis* **139**.
- [17] LEEK, J. T. (2011). Asymptotic Conditional Singular Value Decomposition for High-Dimensional Genomic Data. *Biometrics* **67**.
- [18] MESTRE, X. (2008). Improved Estimation of Eigenvalues and Eigenvectors of Covariance Matrices Using Their Sample Estimates. *IEEE Transactions on Information Theory* **54**.
- [19] PAPADIMITRIOU, S., SUN, J. and FALOUTSOS, C. (2005). Streaming Pattern Discovery in Multiple Time-series. In *Proceedings of the 31st International Conference on Very Large Data Bases*.
- [20] PEDERSEN, H., KOZERKE, S., RINGGAARD, S., NEHRKE, K. and KIM, W. Y. (2009). k-t PCA: Temporally constrained k-t BLAST reconstruction using principal component analysis. *Magnetic Resonance in Medicine* **62**.
- [21] SHARMA, N. and SAROHA, K. (2015). A novel dimensionality reduction method for cancer dataset using PCA and Feature Ranking. In *2015 International Conference on Advances in Computing, Communications and Informatics (ICACCI)*.
- [22] SREBRO, N. and JAAKKOLA, T. (2003). Weighted Low-Rank Approximations. In *Proceedings of the Twentieth International Conference on Machine Learning*.
- [23] TAMUZ, O., MAZEH, T. and ZUCKER, S. (2005). Correcting systematic effects in a large set of photometric light curves. *Monthly Notices of the Royal Astronomical Society* **356**.
- [24] TIPPING, M. E. and BISHOP, C. M. (1999). Probabilistic Principal Component Anal-

- ysis. *Journal of the Royal Statistical Society: Series B (Statistical Methodology)* **61**.
- [25] UDELL, M., HORN, C., ZADEH, R. and BOYD, S. (2016). Generalized low rank models. *Foundations and Trends® in Machine Learning* **9**.
- [26] WAGNER, G. S. and OWENS, T. J. (1996). Signal detection using multi-channel seismic data. *Bulletin of the Seismological Society of America* **86**.
- [27] YOUNG, G. (1941). Maximum likelihood estimation and factor analysis. *Psychometrika* **6**.
- [28] YUE, H. H. and TOMOYASU, M. (2004). Weighted principal component analysis and its applications to improve FDC performance. In *2004 43rd IEEE Conference on Decision and Control (CDC)* **4**.
- [29] ZHANG, A., CAI, T. T. and WU, Y. (2018). Heteroskedastic PCA: Algorithm, Optimality, and Applications. arXiv: 1810.08316.

D. HONG
J. A. FESSLER
L. BALZANO
DEPARTMENT OF ELECTRICAL ENGINEERING
AND COMPUTER SCIENCE
UNIVERSITY OF MICHIGAN
ANN ARBOR, MICHIGAN 48109
E-MAIL: dahong@umich.edu
fessler@umich.edu
girasole@umich.edu